Universität Stuttgart
Geodätisches Institut

Complex Singular Spectrum Analysis of Earth Orientation Time Series

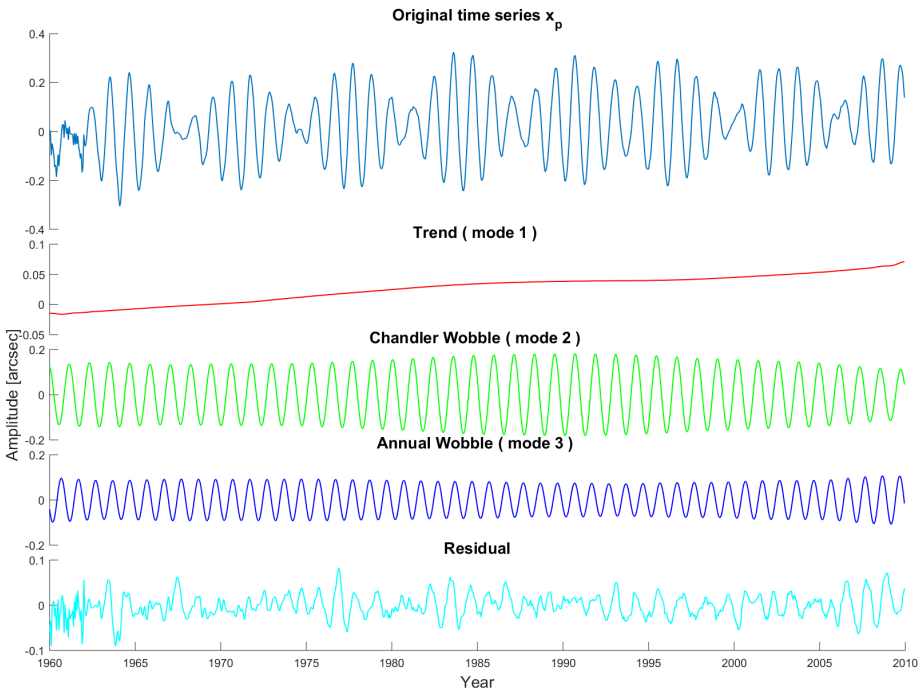

Masterarbeit im Studiengang
Geodäsie und Geoinformatik
an der Universität Stuttgart

Yang LI

Stuttgart, Juli 2018

Betreuer: Prof. Dr.-Ing. Nico Sneeuw
Universität Stuttgart

Erklärung der Urheberschaft

Ich erkläre hiermit an Eides statt, dass ich die vorliegende Arbeit ohne Hilfe Dritter und ohne Benutzung anderer als der angegebenen Hilfsmittel angefertigt habe; die aus fremden Quellen direkt oder indirekt übernommenen Gedanken sind als solche kenntlich gemacht. Die Arbeitwurde bisher in gleicher oder ähnlicher Form in keiner anderen Prüfungsbehörde vorgelegt und auch noch nicht veröffentlicht.

Stuttgart, 20.07.2018
Ort, Datum

Yang Li
Unterschrift

Abstract

The separation of geodetic time series into a sum of a small number of independent and interpretable components is of great importance. Approaches such as Singular Spectrum Analysis (SSA) and Multi-channel Singular Spectrum Analysis (MSSA) have shown their advantage in this field.

The aim of this thesis is to develop theoretical aspects of Complex Singular Spectrum Analysis (CSSA) technique and demonstrate that CSSA can be considered as a powerful method of time series analysis. CSSA is a non-parametric method which extends SSA into bivariate time series analysis technique with complex values.

Using EOP time series in the time period spanning from 1960 to 2009, Chandler wobble (CW), annual wobble (AW) as well as a non-linear trend are successfully separated in both x and y direction by SSA and MSSA. This paper provides evidence for CSSA when performing tasks of EOP time series decomposition. CSSA functions quasi-equivalent with SSA and MSSA of polar motion time series analysis.

Key Words: SSA; MSSA; CSSA; EOP time series

Contents

List of Abbreviations

AW	**A**nnual **W**obble
CSSA	**C**omplex **S**ingular **S**pectrum **A**nalysis
CW	**C**handler **W**obble
EOF	**E**mpirical **O**rthogonal **F**unctions
EOP	**E**arth **O**rientation **P**arameters
ICA	**I**ndependent **C**omponent **A**nalysis
LOD	**L**ength **O**f **D**ay
MSSA	**M**ultivariate **S**ingular **S**pectrum **A**nalysis
RMS	**R**oot**M**ean **S**quare
PC	**P**rincipal **C**omponent
PCA	**P**rincipal **C**omponent **A**nalysis
SSA	**S**ingular **S**pectrum **A**nalysis
SVD	**S**ingular **V**alue **D**ecomposition
UT1	**U**niversal **T**ime

Chapter 1

Introduction

1.1 Motivation

The purpose of time series analysis is to determine some of the system's key properties which can then help understand and predict the system's future behavior by quantifying certain features of the time series (Ghil et al., 2002). In the geodesy, data-driven methods, such as Empirical Orthogonal Function (EOF), Principal Component Analysis (PCA) and Independent Component Analysis (ICA), are used to smooth or model the geodetic time series (Dong et al. (2006); Rangelova et al. (2007); Forootan and Kusche (2012)). Singular Spectrum Analysis (SSA) in its turn is a generalization of PCA and Multi-channel Singular Spectrum Analysis (MSSA) is known as an Extended EOF analysis (Zotov and Shum, 2010).

Over the last two decades, SSA and MSSA have proven their usefulness in the temporal and spatial-temporal analysis of short and noisy time series in several fields of the geosciences and of other disciplines (Ghil et al., 2002).

The starting point of SSA and MSSA is to embed a time series in a vector space, to represent it as a trajectory matrix that generate the time series numerically (Ghil et al., 2002). But SSA can be just used of uni-variate time series analysis. And trajectory matrix for MSSA is too complex. So introduce CSSA whose trajectory matrix is simple and can analyze multivariate time series.

It is worth mentioning these two methods have been shown to be successful in decomposition of polar motion time series into a sum of trend, Chandler wobble, annual wobble and residual.

This thesis is trying to find out a new method, CSSA, to analyze bivariate time series by modelling them as a single-channel complex valued time series. It is important to note that CSSA is used for the first time to analyze polar motion observations. This thesis want to prove that CSSA performs well in multivariate geodetic time series.

1.2 The Earth Orientation Parameters (EOP) time series

The Earth Orientation Parameters (EOP) time series consists of polar motion in x direction x_{p} and y direction y_{p}, Universal Time (UT1), Length of Day (LOD), and celestial pole offsets of precession and nutation. This thesis will analyze polar motion observations from the year 1960 to 2009 both in x and y direction in time domain. It is shown as following:

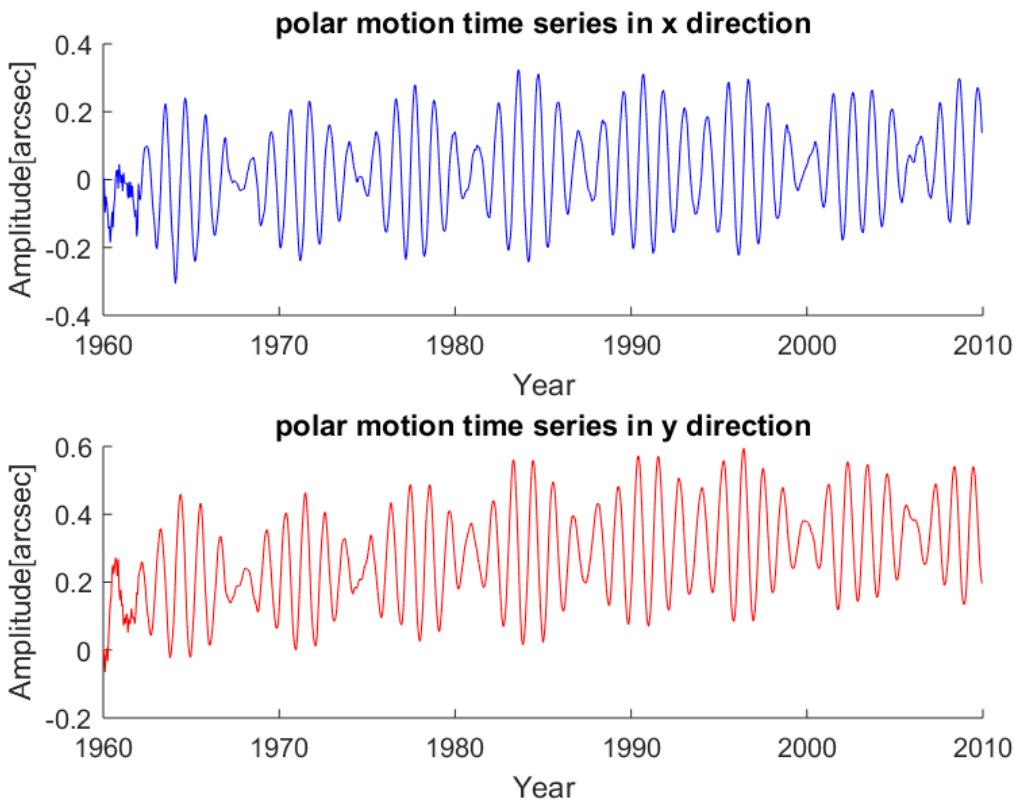

FIGURE 1.1: Polar motion from 1960 to 2009 in x and y direction

Polar motion (or wobble) is the moving of the Earth's rotation axis with respect to the conventional Earth-fixed reference system. Polar motion plays an important role in our understanding of the processes that drive changes in the Earth's rate of rotation to change, solid Earth, atmosphere, and oceans (Malkin and Miller, 2010; Smylie et al., 2015; Höpfner, 2003). It has three major components:

1. A free oscillation called Chandler wobble with period about 435 days.

2. Annual oscillation (annual wobble) forced by the seasonal displacement of air and water masses, beating which each other, give the characteristic pulsating shape of the motion (Vondrák and Richter, 2004).

3. Trend.

The annual oscillation proceeds in the same direction as Chandler wobble with nearly a constant amplitude of about 0.1 $[arcsec]$. The mean pole has an irregular drift in the direction to the $80°$W (Vondrák and Richter, 2004).

This secular motion is mainly due to glacial isostatic adjustment in Canada and Scandinavia, but sea-level changes, large-scale tectonic movements, mass shifts in the Earth's interior and polar ice melting may also contribute to this trend. It is also called polar wander (Torge and Müller, 2012).

Meanwhile there are also some other free motions in addition to Chandler wobble, due to misalignments of rotational axis and figure axes related to the flattened Earth's mantle, and inner and outer core (Torge and Müller, 2012).

These components for free motions will be seen together as residual. There has been some research about the decomposition. These decompositions for polar motion in x direction is shown as following:

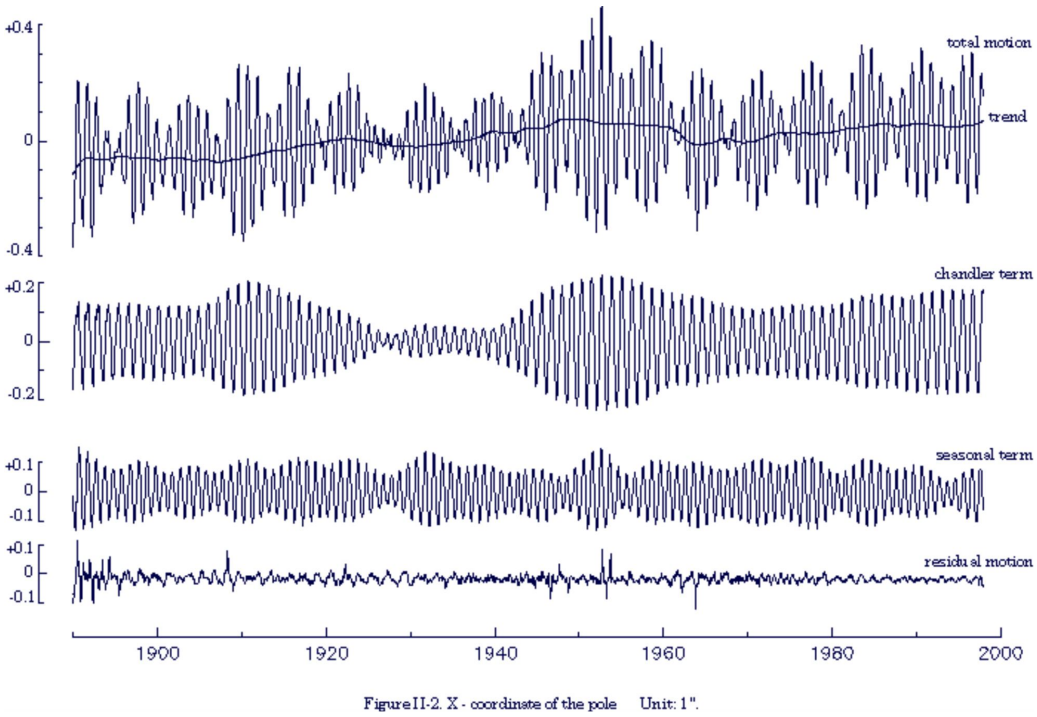

FIGURE 1.2: Polar motion decomposition in x direction.
Source: plot provided by the former Central Bureau. (Created: 1 Jan 2001).
https://www.iers.org/IERS/EN/Science/EarthRotation/Xpole.html?nn=12932.

Decomposition in y direction is shown as following:

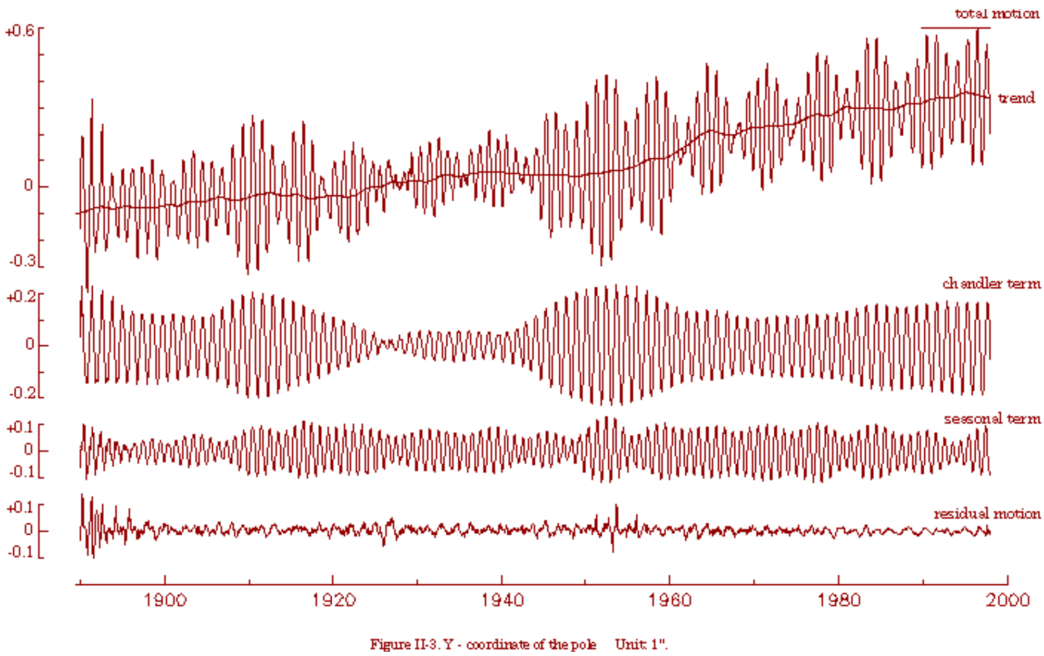

FIGURE 1.3: Polar motion decomposition in y direction.
Source: plot provided by the former Central Bureau. (Created: 1 Jan 2001).
https://www.iers.org/IERS/EN/Science/EarthRotation/Ypole.html?nn=12932.

1.3 Window length choice of window length on polar motion series

As mentioned in section 2, the window length L is the only parameter in the decomposition algorithms of embedding step. So it is really important to choose the proper window length. The selection depends on the objective of the study and on preliminarily information about the time series.

This selection of small values of L has the advantage of increasing the confidence in the results when the objective of the analysis present high frequencies (Oropeza and Sacchi, 2011a). Other authors have said that L has to be sufficiently large so that the main behavior of the time series to analyze is content in each lagged vector (Golyandina et al., 2001) and theoretical results tell us that L should only be large enough but smaller than $N/2$ (Hassani, 2007).

Polar motion time series has two periodic oscillations components with an integer period, for CW with periods of about 435 and AW with 365 days (Höpfner, 2003). Then it is advisable to take the window length proportional to the periods in order to get better

separability of these periodic components (Hassani, 2007). For polar motion time series analysis, in order to separate the oscillations components (CW and AW), also meanwhile the trend, the most appropriate window length L equals 12 to 13 years both in x direction and in y direction (Cui, 2015). As we know from the EOP data set, there are 20 observations per year, so the size of the window length in this thesis will be chosen as 240.

1.4 Structure of thesis

Chapter 1 gives motivation of the thesis with the study history and the application of the methods and introduction of Earth Orientation Parameters (EOP) time series. Then it gives the definition and content of polar motion which is the part we will analyze. What's more, the explanation and pre-knowledge of polar motion are really helpful for the analysis.

The rest of this thesis is organized as follows. In Chapter 2, the introduction for SSA is given first with definition, study history and the usefulness. Then the algorithm of SSA is explained in mathematical formulas. What' more, applying SSA of polar motion time series in x direction and then in y direction. At last, we will do some discussions for the results.

On the other hand, Chapter 3 introduces the expansion of SSA to multiple dimensions called MSSA. Background and algorithm of MSSA are given. And it shows the results for analyzing the polar motion time series both in x and y direction with MSSA. Finally, it gives the discussions on analysis.

Chapter 4 shows background and algorithm of Complex Singular Spectrum Analysis (CSSA) which is expansion of SSA in the complex field. Then it gives results of separating main components from polar motion time series with CSSA and does some discussions on the results got by different generations.

Chapter 5 compares the methods SSA, MSSA with CSSA and show the difference in figures. Then conclusion can be given by the comparison of this three methods. At last, it gives the conclusion and outlook of the whole thesis.

Chapter 2

Singular Spectrum Analysis

This chapter gives the background for Singular Spectrum Analysis (SSA) (Section 2.1) with its history and application, the basic algorithms for SSA with further details on the four main steps (Section 2.2), as well as the emphasizing in its application for decomposing polar motion time series that demonstrate its effectiveness in extracting main components (Section 2.3) and analyzing with amplitude and frequency got by fitting.

2.1 Background

In time series analysis, SSA is a nonparametric spectral estimation method. SSA can be an aid in the decomposition of time series into a sum of a small number of independent and interpretable components such as a slowly varying trend, oscillatory components and a structureless noise, each having a meaningful interpretation (Hassani, 2007). The name "Singular Spectrum Analysis" relates to the spectrum of eigenvalues in a Singular Value Decomposition (SVD) of a covariance matrix, and not directly to a frequency domain decomposition.

SSA are called the Caterpillar method (Golyandina et al., 2001) and Cadzow filtering (Trickett, 2008) in different fields. All this names of methods arise from different fields, but their methods are the equivalent. For instance, the Caterpillar method arises from time series analysis (Nekrutkin, 1996) and the Cadzow method was proposed as a general framework for signal enhancement, denoising images (Cadzow, 1988) and application for random noise attenuation (Trickett, 2008).

Areas where SSA can be applied are very broad: climatology, marine science, geophysics, engineering, image processing, medicine, econometrics (Golyandina et al., 2001). Hence different modifications of SSA have been proposed and different methodologies of SSA are used in practical applications such as trend extraction, periodicity detection, seasonal adjustment, smoothing, noise reduction (Golyandina et al., 2001). It is an important feature of SSA that the trends need not be linear and that the oscillations can be amplitude and phase modulated (Ghil et al., 2002).

The application of SSA consists of two complementary stages with four main steps – embedding, Singular Value Decomposition(SVD), grouping and anti-diagonal averaging. In the next section, the methodology will be explained in detail.

2.2 Methodology

Consider the real-valued time series $Y = (x_1, x_2, x_3, \cdots, x_N)$ of length N. The main purpose of SSA is to decompose the original time series into a sum of independent and interpretable components such as a slowly varying trend, periodic or quasi-periodic components and a structureless noise (Hassani, 2007).

This is followed by two complementary stages: decomposition and reconstruction. In the first stage, we decompose the time series in two steps. The first step is embedding original time series Y with lagged vector X_i into the trajectory matrix $\mathbf{X}$. The second step singular value decomposition represents trajectory matrix $\mathbf{X}$ as a sum of bi-orthogonal elementary matrices $\mathbf{X}_i$ whose rank is one. They will turn polar motion time series into the trend, Chandler wobble, annual wobble and residual according to their singular values. Reconstruction is the second stage. This stage includes two separate steps: grouping and anti-diagonal averaging. We reconstruct the original time series by grouping to make subgroups of the decomposed trajectory matrix and anti-diagonal averaging to reconstruct the new time series from the subgroups. Then it gives algorithm of the SSA technique.

2.2.1 Decomposition

1. First step: Embedding
   In the Basic SSA algorithm applied to a one-dimensional time series
   $Y = (x_1, x_2, x_3, \cdots, x_N)$ of length N. We map the time series Y into the lagged vectors, $X_i = (x_i, x_{i+1}, x_{i+2}, \cdots, x_{i+L-1})$.
   Then build trajectory matrix (Hankel matrix) with equal values on anti-diagonals:

$$\mathbf{X} = \begin{pmatrix} \mathrm{x_1} & \mathrm{x_2} & \cdots & \mathrm{x_L} \\ \mathrm{x_2} & \mathrm{x_3} & \cdots & \mathrm{x_{L+1}} \\ \vdots & \vdots & \ddots & \vdots \\ \mathrm{x_K} & \mathrm{x_{K+1}} & \cdots & \mathrm{x_N} \end{pmatrix}, \tag{2.1}$$

   Where L is lag window length which is the single parameter of the embedding, and $K = N - L + 1$,, with $L < (N+1)/2$. Embedding is a standard procedure in time series analysis (Hassani, 2007).

2. Second step: SVD
Let $S = \mathbf{X}\mathbf{X}^T$, $\lambda_1, \lambda_2, \cdots, \lambda_L$ are eigenvalues of the matrix S. $\sigma_1, \sigma_2, \cdots, \sigma_L$ are the singular values of $\mathbf{X}$ in the decreasing order and $\sigma_i = \sqrt{\lambda_i}$. Let $d = max\{i : \lambda_i > 0\} = rank\mathbf{X}$, $U_1, U_2, \cdots, U_d$ be the corresponding left eigenvectors, and $V_i = \mathbf{X}^T \mathcal{U}_i / \sigma_i, i = 1, 2, \cdots, d$ be right singular vectors. Then the SVD of the trajectory matrix can be written as:

$$\mathbf{X} = \mathbf{X}_1 + \mathbf{X}_2 \cdots \mathbf{X}_d, \tag{2.2}$$

where $\mathbf{X} = U\Sigma\, V^T = \sum_{i=1}^{d} \sigma_i U_i V_i^T, i = 1, 2, \cdots, d$. U_i (called 'factor empirical orthogonal functions' or EOFs) and V_i (called 'principal components') stand for the left and right eigenvectors of $\mathbf{X}$. The collection (Σ_i, U_i and V_i) is called ith $\mathbf{X}$ eigentriple(abbreviated as ET).

2.2.2 Reconstruction

1. First step: Grouping The grouping step corresponds to splitting the elementary matrices $\mathbf{X_i}$ into several groups and summing the matrices within each group (Hassani, 2007). With a set of indices $I = \{i_1, i_2, \ldots, i_p\}$, the matrix $\mathbf{X}_I = \mathbf{X}_{i1} + \ldots \mathbf{X}_{ip}$. The spilt of the set of indices $J = \{1, 2, \ldots, d\}$ into m disjoint subsets $I_1, I_2, \ldots, I_m$, m depends on the type of time series. Each will reflect the properties of initial data components which have a meaningful interpretation. The representation is as follows:

$$\mathbf{X} = \mathbf{X}_{I1} + \ldots \mathbf{X}_{Im}. \tag{2.3}$$

Eigentriple grouping is the procedure to choose the sets $I_1, I_2, \ldots, I_m$.

2. Second step: Anti-diagonal averaging
Each matrix $X_{i,j}$ would be transformed into a new time series from the subgroups of length N at this step. Z is set as the vector as
$Z^{(i)} = \left(z_1^{(i)}, z_2^{(i)}, z_3^{(i)}, \cdots, z_N^{(i)}\right)$, where k is smaller than L. $Z^{(i)}$ is corresponds to the matrix $\mathbf{X}_{Ii}$. Obtain the series by the averaging along anti-diagonals as:

$$z_k^{(i)} = \begin{cases} \frac{1}{k} \sum\limits_{j=1}^{k} x_{j,k-j+1} & 1 \leqslant k < L \\ \frac{1}{L} \sum\limits_{j=1}^{L} x_{j,k-j+1} & L \leqslant k < K+1 \\ \frac{1}{N-k+1} \sum\limits_{j=k-K+1}^{N-k+1} x_{j,k-j+1} & K \leqslant k < N \end{cases} \tag{2.4}$$

Anti-diagonal averaging is applied to produce a reconstructed series
$\mathbf{y} = (y_1, y_2, y_3, \cdots, y_N)$. In this way, the initial series $Y = (y_1, y_2, y_3, \cdots, y_N)$ can be decomposed into a sum of the reconstructed series.

The initial time series $Y = (y_1, y_2, y_3, \cdots, y_N)$ can be reconstructed by

$$y_n = \sum_{i=1}^{m} z_n^{(i)} (n = 1, 2, \cdots, N). \tag{2.5}$$

2.3 SSA of polar motion time series in x direction

Originally, SSA utilized a trajectory matrix of time series in an eigen-spectra decomposition (Vautard and Ghil, 1989). SSA has also been employed to separate between signal and noise component not only for biomedical data but also for economic data (Hassani et al., 2012), estimate time series for signal reconstruction (Golyandina and Stepanov, 2005), in geophysics to study climatic records (Ghil et al., 2002; Chen et al., 2013; Dong et al., 2006; Rangelova et al., 2007), do the seismic data denoising and reconstruction ((Oropeza and Sacchi, 2011a)) and polar motion time series analysis (Miller and Malkin, 2013). However, our focus is its application to polar motion time series analysis in the time period spanning from 1960 to 2009 both in x direction and in y direction on separating main components for trend, Chandler wobble, annual wobble and residual.

x_{p} is polar motion time series in x direction. For polar motion time series analysis, in order to separate the oscillations components (CW and AW), also meanwhile the trend, the most appropriate window length L equals 12 to 13 years both in x direction and in y direction (Cui, 2015). So applying SSA method on x_{p} in these 4 steps with window length of $L = 240$. We choose the first 10 modes to analysis at the beginning to separate the main components for x_{p}.

2.3.1 Decomposition first 10 modes

Applying SSA method on x_{p} time series. As a result, modes according to singular values are in the decreasing order. So there shows decomposition result of the first 10 modes. The plot is as following:

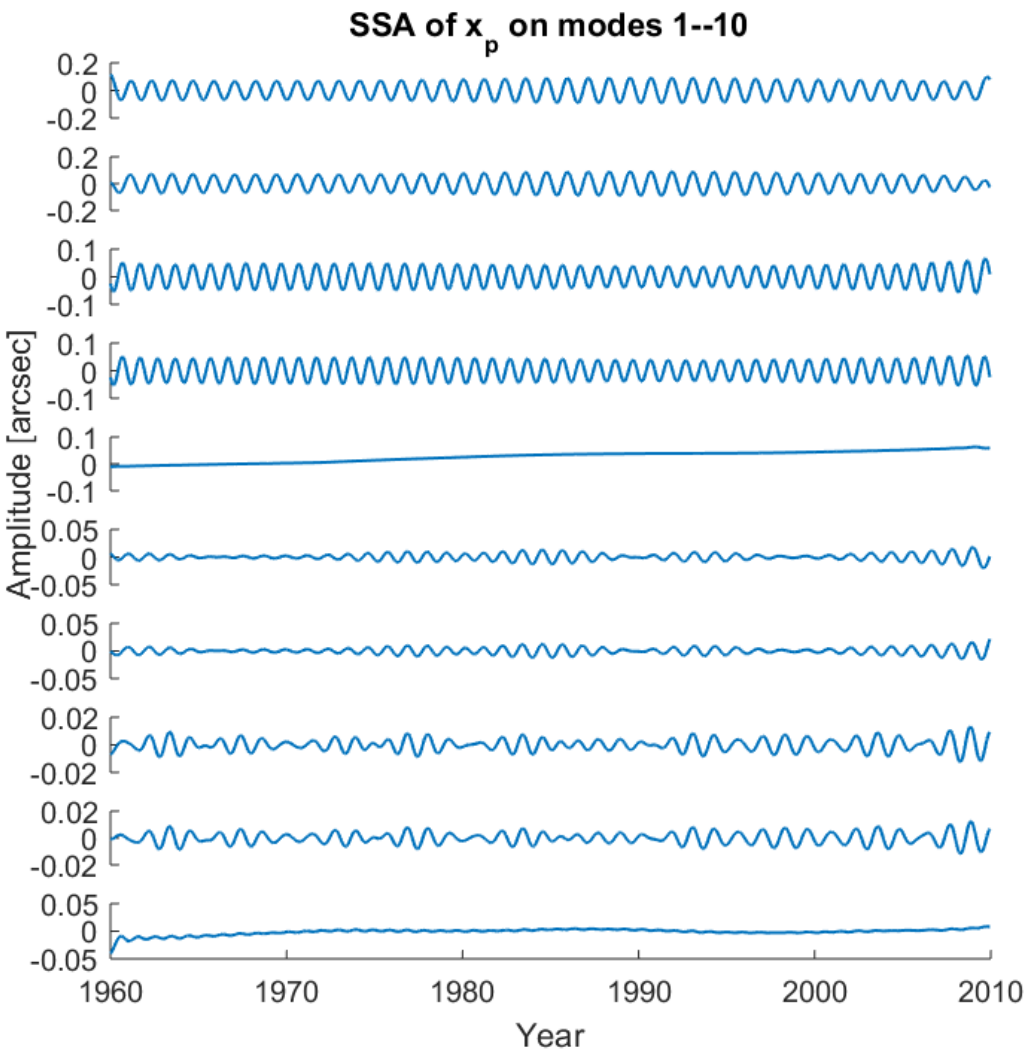

FIGURE 2.1: Reconstructed modes 1–10 of x_{p} by SSA

In order to separate the reconstructed modes into different components, plot x_{p} amplitudes of oscillatory components as following:

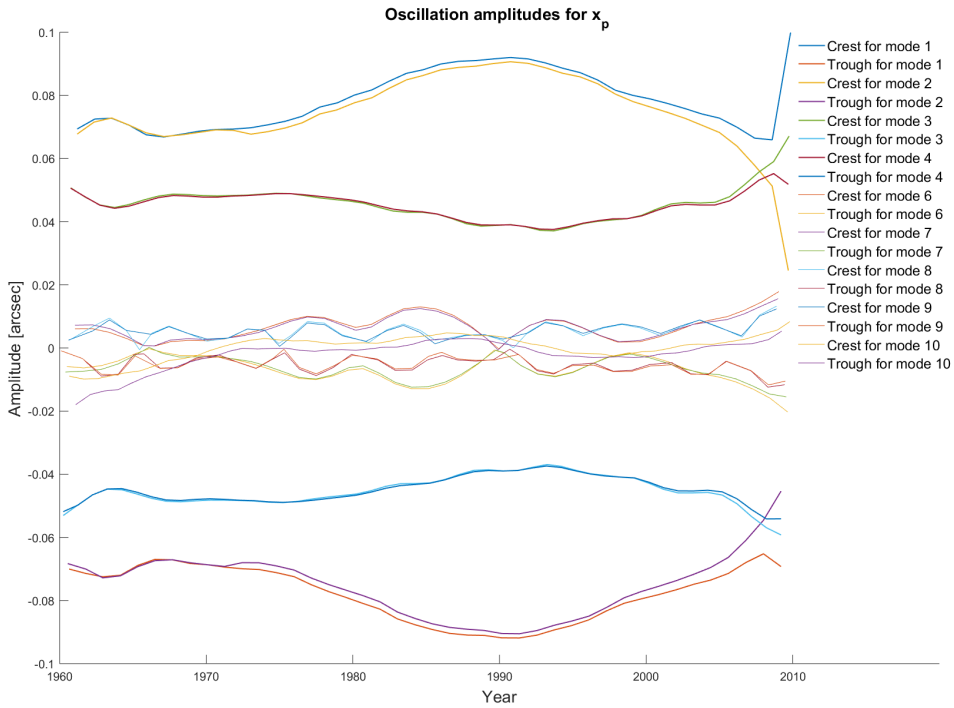

FIGURE 2.2: x_{p} amplitudes on SSA reconstructed modes

As shown in the figure.2.2, the reconstructed mode 1, mode 2, mode 3 and mode 4 represent the main oscillatory components. In order to show the amplitude and frequency, use the curve fitting method 'Sum of Sine' (in cftool of Matlab) to fit the main oscillatory components in number of terms of 1. The fitting equation is shown as: $f = a_1 \sin(b_1 t + c_1))$, where a_1 is amplitude, b_1 is frequency, c_1 is phase and t is time. As a result, we get the curve fitting parameters as follows:

TABLE 2.1: Oscillatory modes' fitting parameters for x_{p} by SSA

fitting parameter	a_1 $[arcsec]$	b_1 $[rad/year]$	c_1 $[rad]$
mode 1	0.078 02	5.301	-44.83
mode 2	0.0744	5.304	-39.79
mode 3	0.045 49	6.289	-0.9006
mode 4	0.045 08	6.289	-2.491

1. Even if we do not have the priori information about these data, it is possible to conclude that the first four modes reconstructions corresponding to the first four singular values represent the main oscillatory components of the time series.

2. It is easily to figure out from figure.2.2 that both of them are the strongest components (mostly from 0.07 $[arcsec]$ to 0.1 $[arcsec]$) among all Reconstructed mode. Besides, from the table below, it is obvious that reconstructed mode 1 and mode 2 for x_{p} have almost the same curve fitting frequency (5.301 $[rad/year]$ for mode 1 and 5.304 $[rad/year]$ for mode 2) and amplitude ($0.078\,02$ $[arcsec]$ for mode 1 and 0.0744 $[arcsec]$ for mode 2). As a result, the reconstructed mode 1 and mode 2 are seen as the same component and grouped into one component.

3. x_{p} reconstructed mode 3 and mode 4 are also oscillatory components but with smaller amplitude compared with mode 1 and mode 2. The amplitude curves of mode 3 and mode 4 are close in 2.2. The amplitudes are from 0.04 $[arcsec]$ to 0.06 $[arcsec]$. As shown in 2.1, the frequency of mode 3 is 6.289 $[rad/year]$ and the same as mode 4 which is higher than mode 1 and mode 2. As a result, reconstructed mode 3 and mode 4 are considered as the same oscillatory reconstruction component but different from the first two.

4. Reconstructed mode 5 for x_{p} in 2.1 is quite different from the rest of the first 10 modes. It is not a periodic signal but a trend. Meanwhile it is quite strong with continuous semi-linear feature, so it should be seen as one main component.

5. Reconstructed mode 6 for x_{p} is not trend but oscillation. But the amplitude is obviously smaller than the mode 1 to 4 and the period is not recognized. So it is neither periodic time series nor trend. So as the other modes. So it is not meaningful to study on these reconstructed components. The amplitude is smaller than 0.02 $[arcsec]$ corresponding to the small singular values. They are neither periodic time series nor trend. As for the polar motion time series analysis, it is not important to study on these reconstructed components. So we just regard all the left part without mode 1 to mode 5 as residual.

2.3.2 Reconstruction main components

Group the x_{p} reconstructed mode 1 and mode 2 as CW, mode 3 and mode 4 as AW, other modes as residual. Reconstructed mode 5 is seen as trend. The main components are shown as:

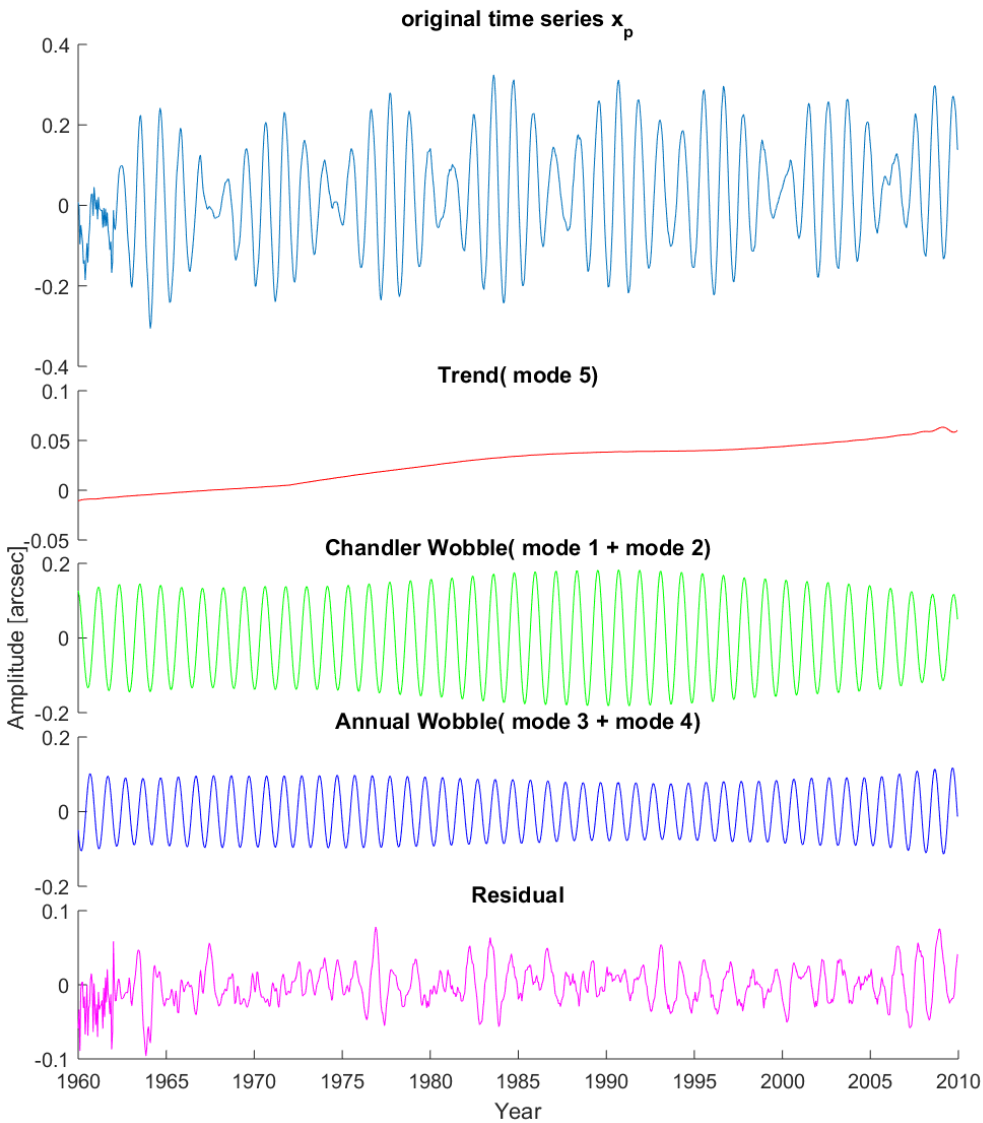

FIGURE 2.3: Main reconstructed components for x_{p} by SSA

CW and AW are reconstructed by grouping modes. In oder to analyze them, we got the curve fitting parameters by curve fitting method with equation 2.3.1.

TABLE 2.2: Reconstructed components' fitting parameters for x_{p} by SSA

fitting parameter	a_1 $[arcsec]$	b_1 $[rad/year]$	c_1 $[rad]$
CW	0.1524	5.306	-42.39
AW	$0.090\,57$	6.289	-1.684

1. The first sub-figure of figure.2.3 is the original polar motion time series in x direction. The second one from reconstructed mode 5 of x_{p} is semi-linear and non-periodic. It is recognized as trend.

2. The sum reconstructed mode 1 and mode 2 is seen as CW in the polar motion time series analysis. The result is shown in the third sub-figure below. The fitting frequency of CW for x_p is 5.306[Hz]. The equation to calculate the period is: $T = \dfrac{2\pi}{f}$. So period of CW is $1.184\,166$ $[year]$ which is 432.457 days. As explained polar Motion time series in 1, the period of CW is about 435 days (Höpfner, 2003). It is almost the similar to the period of CW, so the reconstruction of the CW by SSA is credible.

3. The sum of x_p reconstructed mode 3 and mode 4 are shown in the fourth sub-figure. It is seen as the AW. Its amplitude by fitting is $0.090\,57$ $[arcsec]$ and period calculated by equation2 is 0.999 $[year]$. As we know, the period of AW is $1year$ and the amplitude is 0.1 $[arcsec]$ (Höpfner, 2003). So SSA is a feasible method for separating the AW from the x_p polar motion time series.

4. Residual of x_{p} is shown in the last one. It is the sum of the left reconstructed modes whose amplitude is smaller than 0.02 $[arcsec]$. They are not periodic time series or a trend. So we see them as residual.

2.4 SSA of polar motion time series in y direction

y_{p} is the polar motion time series in y direction. Applying SSA methods on y_{p} with the 4 steps with the window length of $L = 240$. As we know that singular value in the decreasing order, just choose the first 10 modes to analysis at the beginning to separate the main components.

2.4.1 Decomposition first 10 modes

Applying SSA on y_{p} time series and show the result of the first 10 modes corresponding to the singular values. The plot is as following:

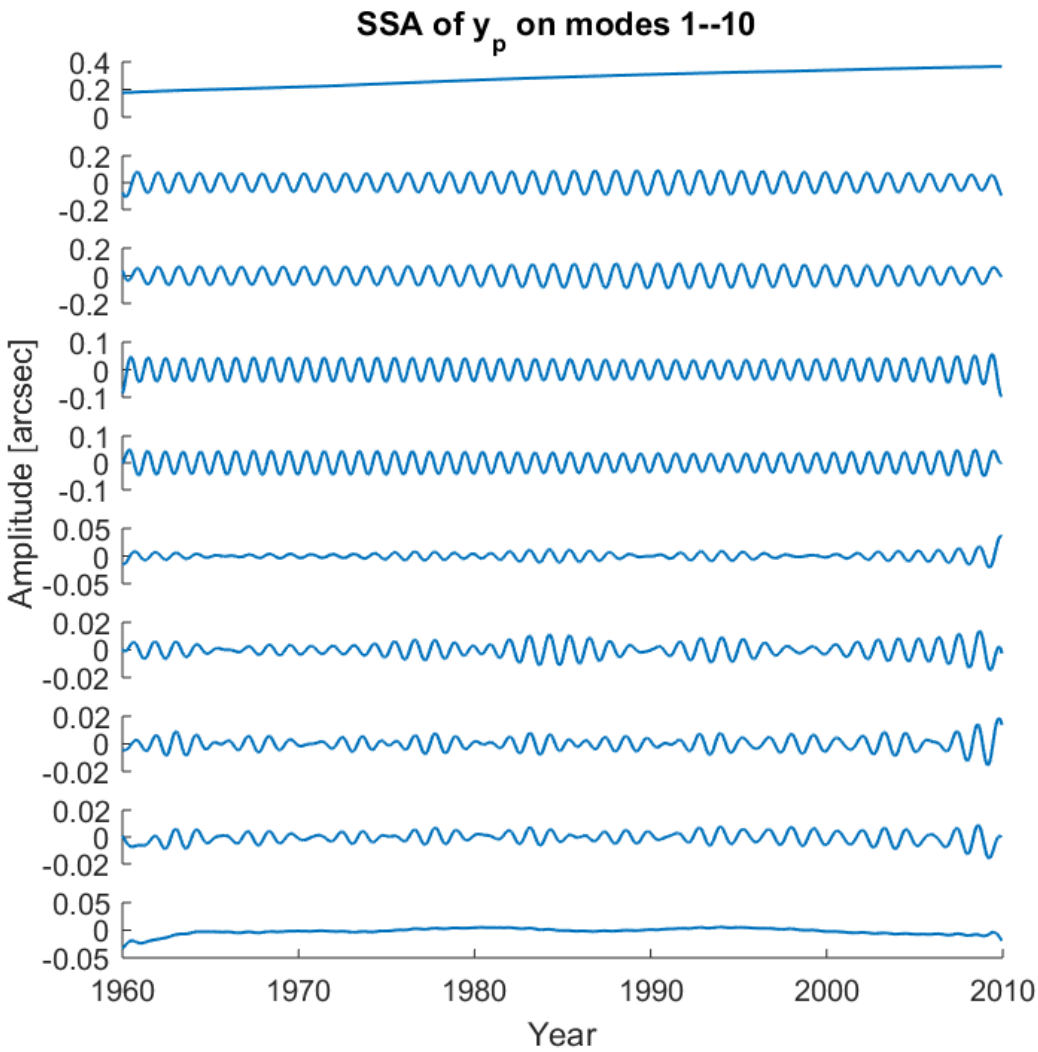

FIGURE 2.4: Reconstructed modes 1–10 of y_{p} by SSA

In order to select the main components from the all reconstructed modes, we plot the amplitudes of the oscillatory components. The y_{p} amplitude of oscillatory modes shows as following:

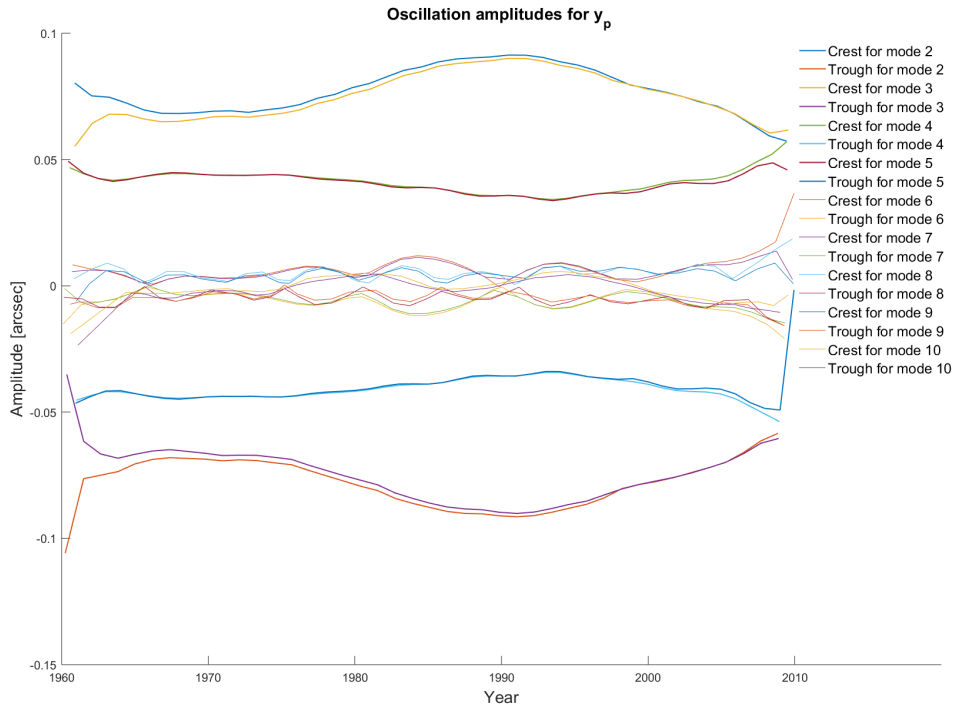

FIGURE 2.5: y_p amplitudes on SSA reconstructed modes

In order to show the amplitude and frequency of y_{p} main oscillatory components, we use the same curve fitting method of 2.3.1 as x_{p}. As a result, we get the fitting parameters as following:

TABLE 2.3: Oscillatory modes' fitting parameters for y_{p} by SSA

fitting parameter	a_1 $[arcsec]$	$b_1[rad/year]$	c_1 $[rad]$
mode 2	0.077 752	5.305	-40.17
mode 3	0.073 54	5.303	-41.62
mode 4	0.041 98	6.293	-8.397
mode 5	0.040 31	6.287	4.595

1. It can be easily figure out that the first reconstructed mode with the biggest singular value represents trend.

   y_{p} reconstructed mode 1 in figure.2.4 is semi-linear with a strong feature for continuous growing up. It is easy to differ the mode 1 from the rest of the first 10 modes. So reconstructed mode 1 is seen as the main component for trend. The following four modes reconstruction represent the main oscillatory components of y_{p} time series.

2. The amplitude curve in figure.2.5 of reconstructed mode 2 and mode 3 for y_{p} looks quite similar. It is obvious that they are the strongest components among all reconstructed modes. Fitting amplitude for mode 2 is $0.077\,752$ $[arcsec]$ and the frequency is 5.305 $[rad/year]$. For mode 3, fitting amplitude is $0.073\,54$ $[arcsec]$ and frequency is 5.303 $[rad/year]$. With almost the same oscillations and amplitude, we see them as one component and the reconstructed mode 2 and mode 3 can be grouped into one component.

3. In figure.2.4, reconstructed mode 4 and mode 5 for y_p are also oscillatory components like mode 2 and mode 3 but with smaller amplitudes. As shown in figure.2.3, the fitting amplitude for mode 3 and mode 4 are around 0.04 $[arcsec]$ and frequency around 6.29 $[rad/year]$. As a result, they are considered as the same reconstruction component.

4. y_{p} reconstructed mode 6 in figure.2.4 is not trend but oscillation. The amplitude is obviously smaller than the mode 2 to 4 and the period is not recognized. So it is neither periodic time series nor trend. As for polar motion time series analysis, it is not important to study on these reconstructed components because of the small amplitude. So as the left reconstructed modes. So we just regard all the left part without mode 1 to mode 5 as residual.

2.4.2 Reconstruction main components

Reconstructed mode 1 for y_p is seen as trend. Group the mode 2 and mode 3 as CW, mode 4 and mode 5 as AW, other modes as residual. The main components are shown as :

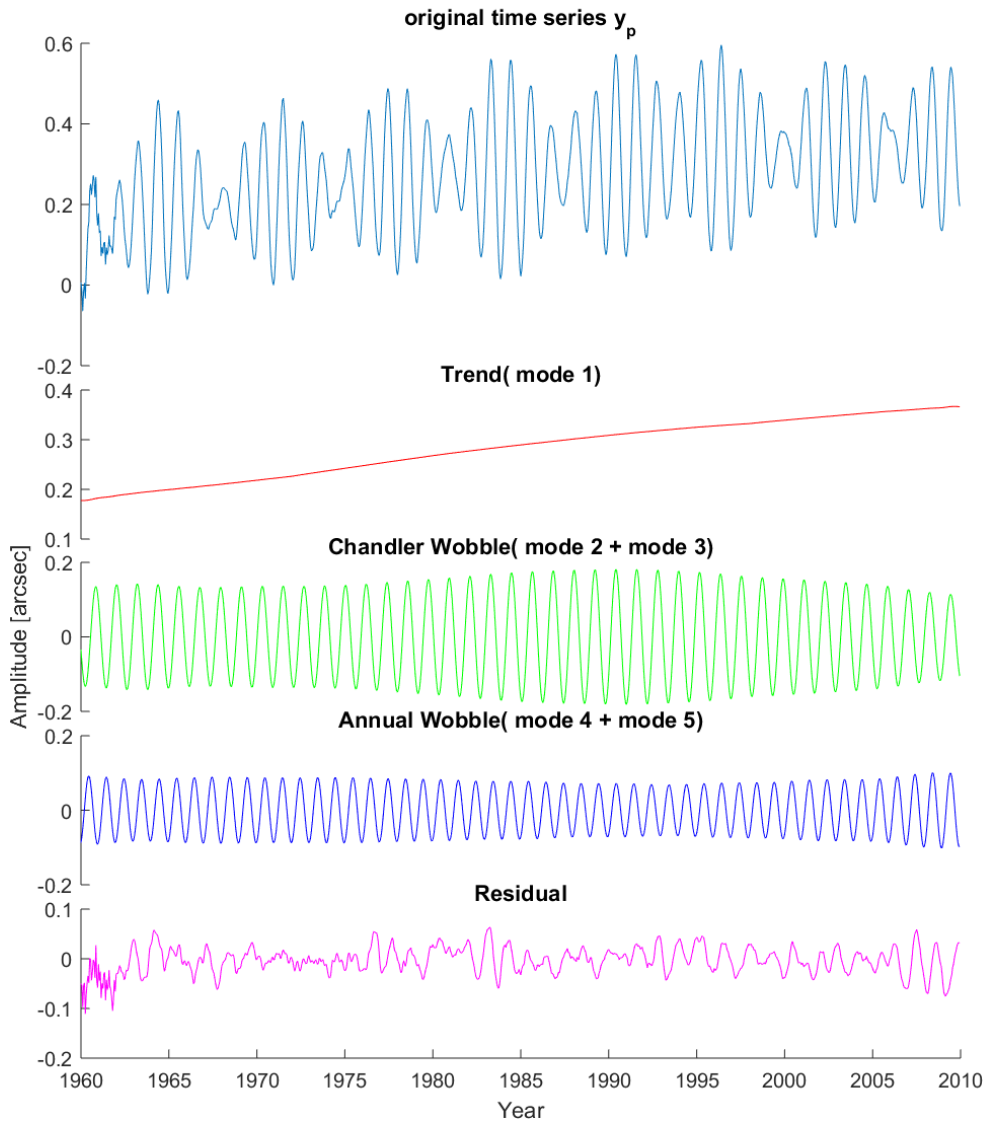

FIGURE 2.6: Main reconstructed components for y_p by SSA

CW and AW are reconstructed by grouping modes. In oder to analyze them, fit by curve fitting method of 2.3.1 to get the fitting amplitude and frequency.

TABLE 2.4: Main reconstructed components for y_{p} by SSA

fitting parameter	a_1 $[arcsec]$	b_1 $[rad/year]$	c_1 $[rad]$
CW	0.151	5.304	-43.99
AW	0.0822	6.29	-2.21

1. Original polar motion time series y_{p} shows in the first sub-figure of figure.2.6. The second one shows trend which is from reconstructed mode 1 for y_{p}. It is semi-linear and non-periodic. Compared with figure.2.2 the trend for x_p, the singular value for y_{p} is bigger so the slope of the trend is larger and the tendency in the figure is more obvious. This is verified by the original time series in the first sub-figure.

2. The sum of reconstructed mode 2 and mode 3 for y_p is shown in the third sub-figure. It is seen as CW in the polar motion time series analysis. We get the fitting amplitude and frequency by cftool within the equation of 2.3.1. Within the fitting frequency, calculate the period of CW by 2. Then we get the fitting period result for $1.184\,613$ $[year]$ which is 432.621 days.

3. The sum of reconstructed mode 4 and mode 5 for y_{p} is shown in the fourth sub-figure. It is seen as the AW. Its fitting amplitude is around 0.822 $[arcsec]$ and period calculated by the equation 2 is $0.998\,92$ $[year]$. It is an annual oscillation.

4. Residual of y_{p} is shown in the last one of the 2.6. The amplitudes for reconstructed mode 6 until the last mode are small. So we sum all the left reconstructed modes without the fist 5 modes as residual. It is not periodic time series or a trend.

5. As we explain in 1, the period of CW is about 435 days (Höpfner, 2003). The fitting result of CW which is reconstructed by SSA method is 432.621 days. It is almost the same as the period of CW. The period of AW is 1 $[year]$ and the amplitude is 0.1 $[arcsec]$ (Höpfner, 2003). The fitting result of AW which is reconstructed by SSA method is $0.998\,92$ $[year]$. The periods of AW are almost same. As a result, it is reliable to separate the CW and AW from polar motion time series by SSA method.

Chapter 3

Multi-channel Singular Spectrum Analysis

A significant improvement on the application of SSA in 2 arises from its expansion to multiple dimensions, which is called Multi-channel Singular Spectrum Analysis (MSSA) (Oropeza and Sacchi, 2011a). This chapter gives the background with its history and application for MSSA (Section 3.1), the basic algorithms for MSSA with further details in mathematical equations on the four main steps (Section 3.2), as well as the emphasizing in its application for decomposing polar Motion time series that demonstrate its effectiveness in extracting main components (Section 3.3) and some discussions.

3.1 Background

Multi-channel, Multivariate SSA (or MSSA), is a time series analysis method (Read, 1993). It is also known as an Extended Empirical Orthogonal Functions (EEOF) analysis (von Storch and Zwiers, 2002), is a generalization of the SSA over the multidimensional time series (Zotov and Shum, 2010), where the size of different univariate series does not have to be the same. They are both the extensions of classical PCA which is actually a special case of the MSSA when no time lags are introduced (Chen et al., 2013). The trajectory matrix of multi-channel time series consists of stacked trajectory matrices of separate times series. The rest of the algorithm is the same as in the univariate case. System of series can be forecasted analogously to SSA recurrent and vector algorithms (Golyandina and Stepanov, 2005).

MSSA provides insight into the unknown or partially known dynamics of the underlying system by decomposing the delay-coordinate phase space of a given multivariate time series into a set of data-adaptive orthonormal components. These components can be classified essentially into trend, oscillatory patterns and noises (Groth and Ghil, 2011).

It has been applied to intraseasonal variability of large-scale atmospheric fields for predicting climate records (Mo, 2001). Besides, it shows the advantage of reconstruction and denoising on geodetic data (Zotov and Shum, 2010, Oropeza and Sacchi, 2011b and

Golyandina and Stepanov, 2005) and decomposing the dynamic time series (Groth and Ghil, 2011).

3.2 Methodology

Consider the multi-channel time series $Y = x_d(n) : d = 1, \ldots, D, n = 1, \ldots, N$ be a multivariate time series with D channels of length N. There are three steps. The first step is embedding original time series Y with lagged vector $X_d(i)$ into the trajectory matrix $\mathbf{X}$. The second step is building covariance matrix to get eigenelements for principal components. The second step is reconstruction of the time series. Polar motion time series can be separated into the trend, Chandler wobble, annual wobble and residual by MSSA. Then it gives algorithm for MSSA.

3.2.1 Embedding

We map time series $Y = x_d(n) : d = 1, \ldots, D, n = 1, \ldots, N$ into the lagged vectors, $X_d(i) = (x_d(i), x_d(i+1), x_d(i+2), \cdots, x_d(i+L-1))$. Then build trajectory matrix (Hankel matrix) which is DM columns of length $N - L + 1$ with equal values on anti-diagonals as following:

$$\mathbf{X} = \begin{pmatrix} x_1(1) & x_1(2) & \cdots & x_1(L) & & x_D(1) & x_D(2) & \cdots & x_D(L) \\ x_1(2) & x_1(3) & \cdots & x_1(L+1) & & x_D(2) & x_D(3) & \cdots & x_D(L+1) \\ \vdots & \vdots & \ddots & \vdots & \cdots & \vdots & \vdots & \ddots & \vdots \\ x_1(K) & x_1(K+1) & \cdots & x_1(N) & & x_D(K) & x_D(K+1) & \cdots & x_D(N) \end{pmatrix}, \tag{3.1}$$

Where L is lag window length which is the single parameter of the embedding, and $K = N - L + 1$,, with $L < (N+1)/2$.

3.2.2 Covariance matrix

1. Calculate the grand covariance matrix $C_{\mathbf{X}}$,

$$C_{\mathbf{X}} = \frac{1}{N}\mathbf{X}^T\mathbf{X}. \tag{3.2}$$

2. Diagonalized covariance matrix $C_{\mathbf{X}}$,

$$\Lambda = Q^T C_{\mathbf{X}} Q. \tag{3.3}$$

A diagonal matrix Λ contains the real eigenvalues λ_k of $C_{\mathbf{X}}$, and a matrix Q whose columns are the associated eigenvectors e_k.

3. Principal components Projecting the trajectory $\mathbf{X}$ onto the eigenvectors,

$$A = \mathbf{X}E, \tag{3.4}$$

the entries of the PC matrix A can be written in a_k,

$$a_k(n) = \sum_{d=1}^{D} \sum_{l=1}^{L} x_d(n+l-1)\, e_{dk}(l), \tag{3.5}$$

with $k = 1, \ldots, DL$, and $n = 1, \ldots, N - L + 1$.

3.2.3 Reconstruction

$$r_{dk}(n) = \frac{1}{M_n} \sum_{l=L_n}^{U_n} a_k(n-l+1)\, e_{dk}(l), \tag{3.6}$$

where e_{dk} associated eigenvectors at d channel. The r_{dk} are referred to as reconstructed components and represent that part of channel x_d that corresponds to the eigenelement pair (λ_k, e_k). The values of the normalization factor M_n and the summation bounds L_n and U_n for the central part of the time series.

3.3 MSSA of bivariate polar motion time series

MSSA method is often applied to multi-components seismic data denoising and the missing values reconstruction ((Oropeza and Sacchi, 2011b)), to study gravity field ((Zotov and Shum, 2010)) and to forecast in the econometric field ((Zhigljavskya et al., 2008)). However, our focus is analyzing polar motion time series analysis x_{p} in x direction and y_{p} in y direction at the same time in the time period spanning from 1960 to 2009 by MSSA and separating main components as trend, CW, AW and residual for x_{p} and y_{p}.

3.3.1 Separation of x_{p} time series

Decomposition of first 10 modes

Applying MSSA method on x_{p} time series and plot the result of the first 10 modes corresponding to the singular values as following:

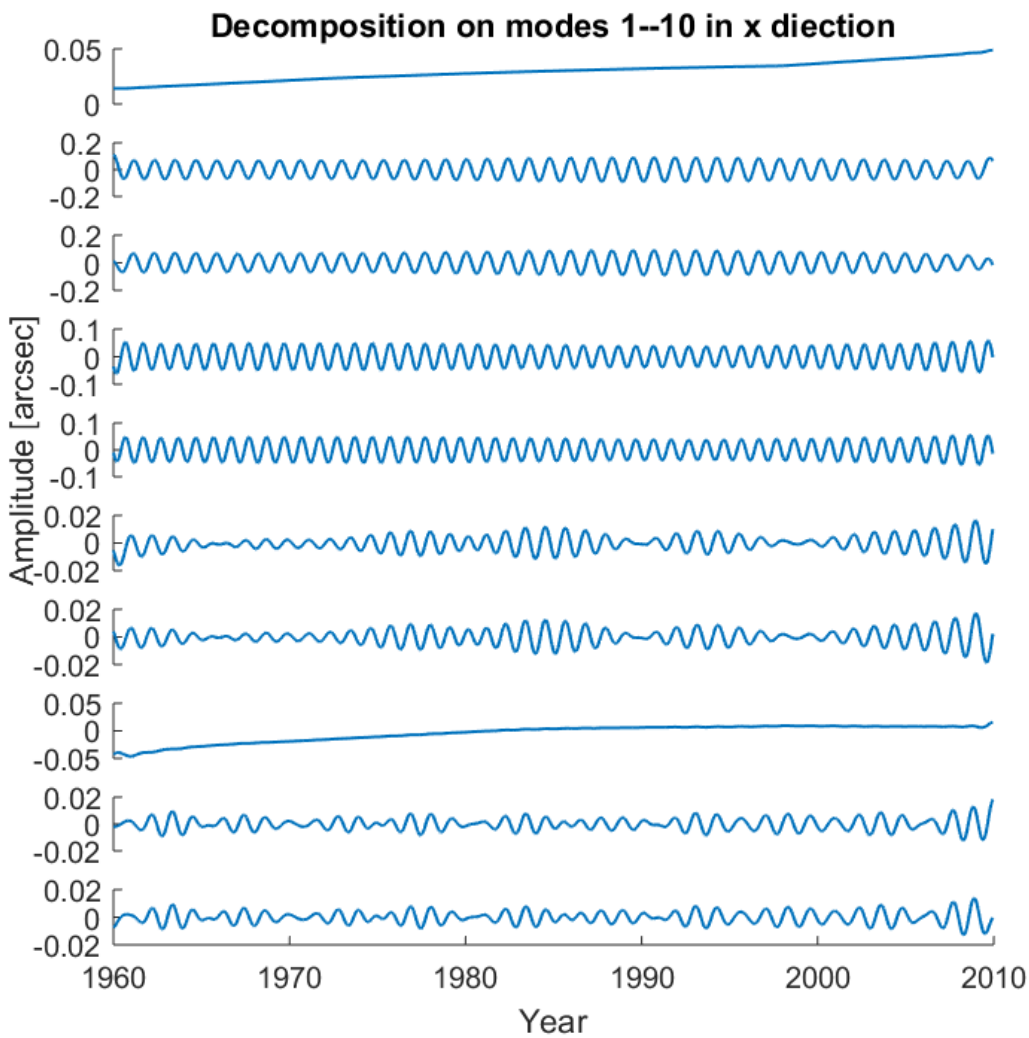

FIGURE 3.1: Reconstructed modes 1–10 of x_{p} by MSSA

In order to separate the reconstructed modes into different components, plot x_p amplitude of main oscillatory components as following:

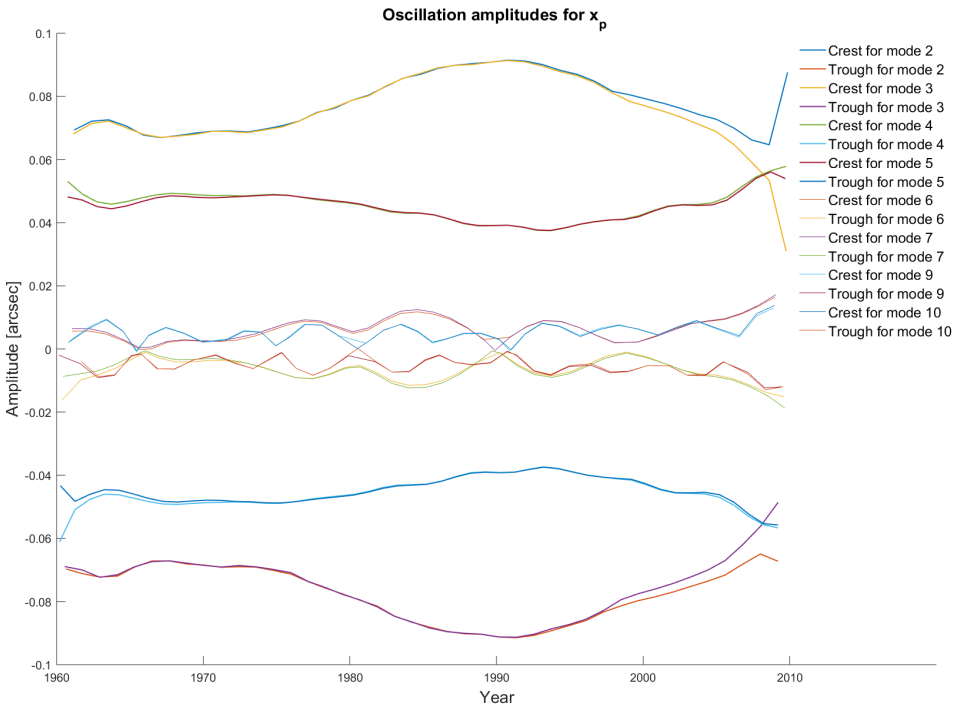

FIGURE 3.2: x_{p} amplitudes on MSSA reconstructed modes

In order to show the amplitude and frequency, we use the same curve fitting method applied in MSSA to show main oscillatory components. As a result, fitting parameters as following:

TABLE 3.1: Oscillatory modes' fitting parameters for x_p by MSSA

fitting parameter	a_1 $[arcsec]$	b_1 $[rad/year]$	c_1 $[rad]$
mode 2	0.077 41	5.306	-43.67
mode 3	0.075 1	5.304	-38.48
mode 4	0.04566	6.289	-1.451
mode 5	0.04506	6.29	-2.99

1. It is obvious that reconstructed both mode 1 and mode 8 for x_{p} in figure.3.1 is trend. They are quite different from rest of the first 10 modes which are oscillation. Meanwhile they are quite strong with continuous semi-linear feature, so they should be the same main component for x_{p}.

2. From figure.3.2, we can see that reconstructed mode 2, mode 3, mode 4 and mode 5 are the main oscillatory components of time series x_{p} with stronger amplitudes. So we fit the curve with 'cftool' in Matlab to get fitting parameters shown in table.3.1.

3. As shown in figure.3.2, amplitudes for reconstructed mode 2 and mode 3 for x_p by MSSA are almost the same. Fitting frequency for mode 2 is 5.306 $[rad/year]$ and for mode 3 is 5.306 $[rad/year]$. As a result, the reconstructed mode 2 and 3 can be grouped in one component.

4. x_{p} reconstructed mode 4 and mode 5 are also oscillatory components with nearby amplitudes. Their amplitudes are between 0.04 $[arcsec]$ and 0.06 $[arcsec]$. As a result, they are considered as the same reconstruction component. Compared with reconstructed mode 2 and mode 3, the fitting amplitude are smaller and frequencies are higher. So reconstructed component for mode 4 and mode 5 are seen as the other different oscillatory component from the mode 2 and mode 3.

5. Reconstructed mode 6, mode 7, mode 9 and mode 10 for x_p are not trend but oscillation. But the amplitudes are obviously smaller than 0.02 $[arcsec]$ and the period is not recognizable. So it is neither periodic time series nor trend. It is not meaningful to study on these reconstructed components. So we just regard all the left part without mode 1, mode 2, mode 3, mode 4, mode 5 and mode 8 as residual.

Reconstruction main components of x_{p} by grouping

Group the MSSA reconstructed mode 2 and mode 3 for x_{p} as CW, mode 4 and mode 5 as AW, other modes as residual. Reconstructed mode 1 and mode 8 are seen as trend. The main components are shown as following:

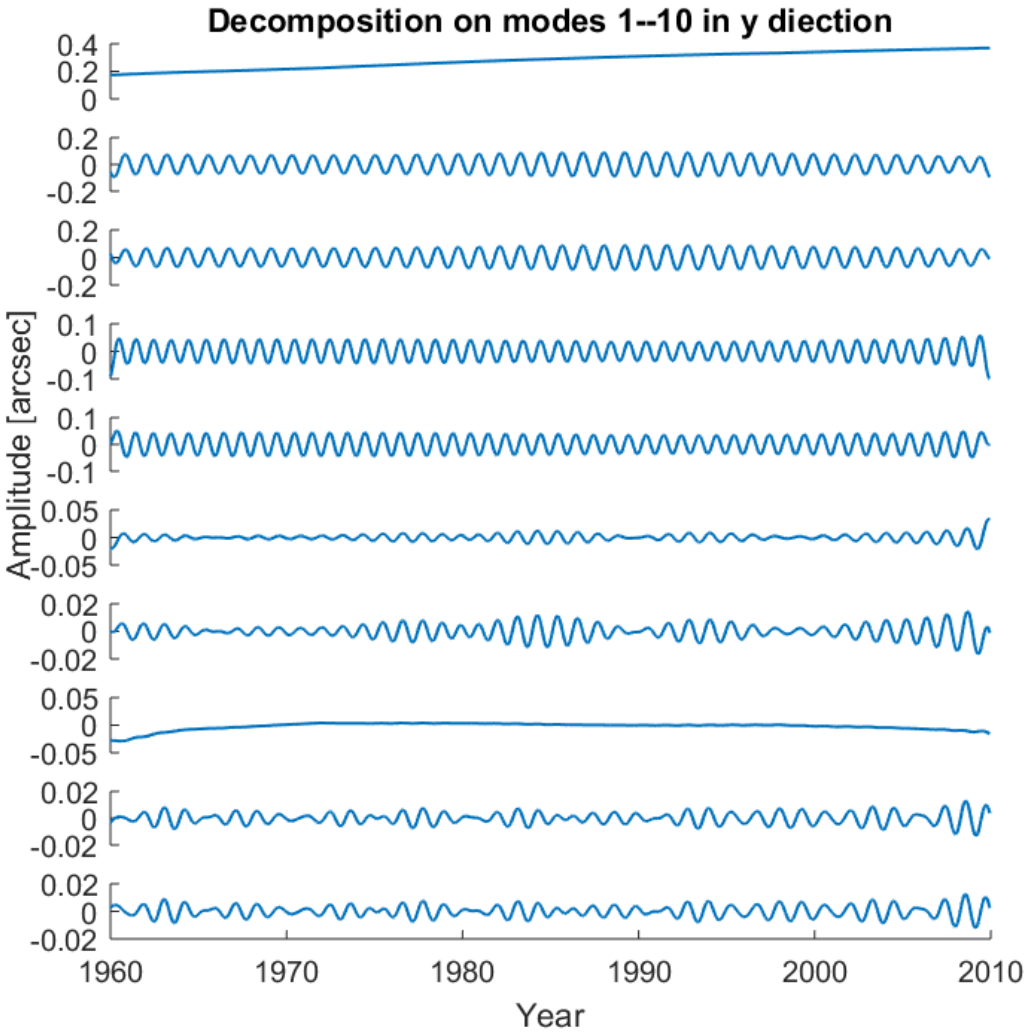

FIGURE 3.3: Main reconstructed components for x_{p} by MSSA

CW and AW are reconstructed by grouping modes. In oder to analyze them, we get the fitting parameters for MSSA reconstructed components by curve fitting method of equation.2.3.1.

TABLE 3.2: Reconstructed components' fitting parameters for x_{p} by MSSA

fitting parameter	a_1 $[arcsec]$	b_1 $[rad/year]$	c_1 $[rad]$
CW	0.1524	5.305	-41.13
AW	0.090 71	6.289	-2.207

1. The first sub-figure of figure.3.3 is the original time series x_{p}. The second one from is semi-linear and non-periodic. It is reconstructed by summing mode 1 and mode 8 and recognized as trend.

2. CW for x_{p} is reconstructed by summing mode 2 and mode 3. The grouping result is shown in the third sub-figure below. The fitting amplitude for reconstructed CW is 0.1524 $[arcsec]$ and frequency is 5.305 $[rad/year]$. As we know frequency, the period for CW can be calculate by $T = \frac{2\pi}{f}$. So period of reconstructed CW is 432.5389 days. As explained polar motion time series in 1, the period of Chandler Wobble is about 435 days (Höpfner, 2003). It is almost the same as the period of CW, so it is a good idea to reconstruct CW for x_{p} by MSSA .

3. AW is grouped by the sum of x_p reconstructed mode 4 and mode 5 which is shown in the fourth sub-figure. Its fitting amplitude is $0.090\,71$ $[arcsec]$ and frequency is 6.289 $[rad/year]$. So the period for reconstructed AW calculated by equation.2 is 0.999 $[year]$. As we know, the period of AW is 1 $[year]$ and the amplitude is 0.1 $[arcsec]$ (Höpfner, 2003). So MSSA is also a good choice for separating the AW for x_{p}.

4. Residual of x_{p} is shown in the last one. It is the sum of the left reconstructed modes whose amplitude is small. They are not periodic time series or a trend. So we see them as residual.

3.3.2 Separation of y_{p} time series

Applying MSSA on y_{p} time series and show the result of the first 10 modes corresponding to the singular values. The plot is as following:

Decomposition of first 10 modes

Applying MSSA on y_{p} time series and show the result of the first 10 modes corresponding to the singular values. The plot is as following:

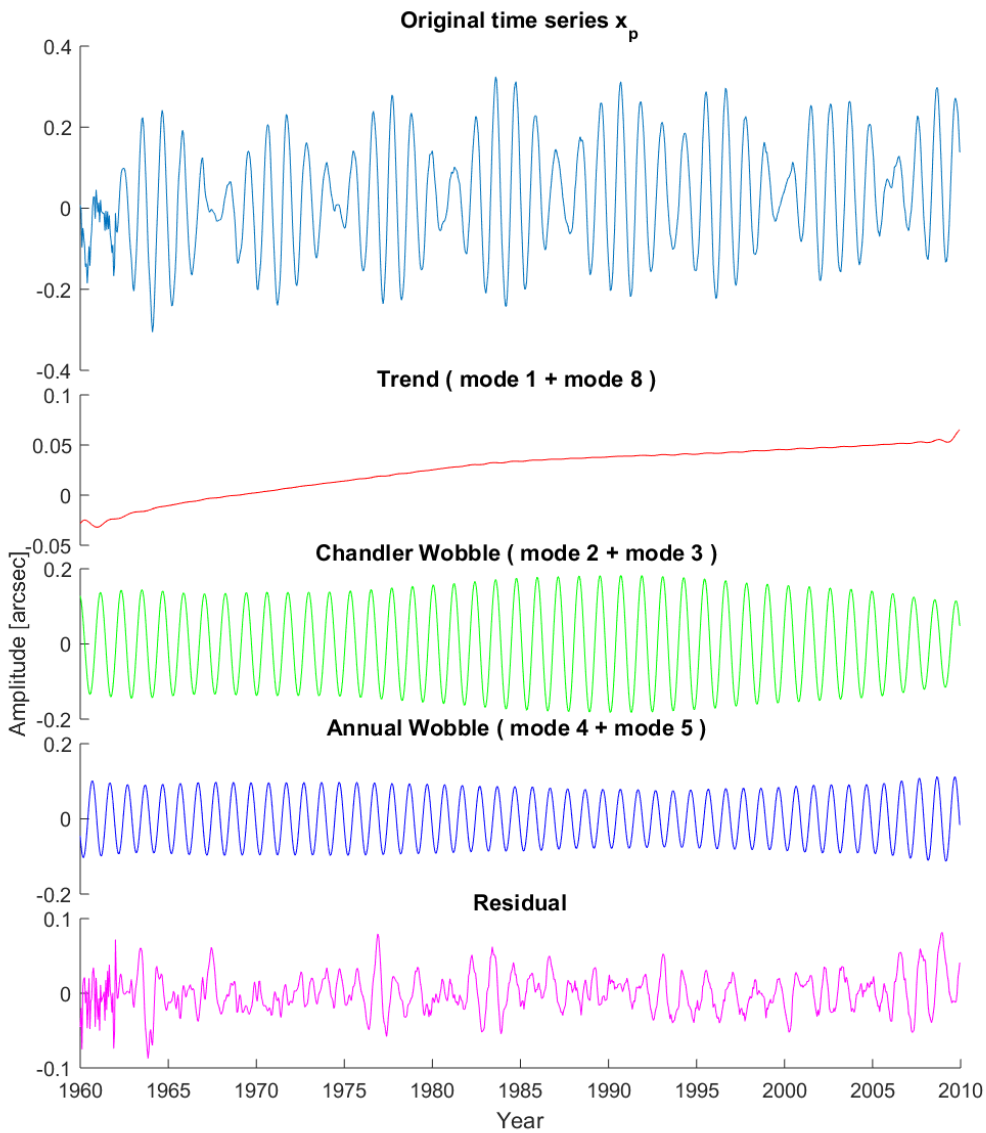

FIGURE 3.4: Reconstructed modes 1–10 of y_{p} by MSSA

Amplitude of oscillatory components for y_{p} shows as following:

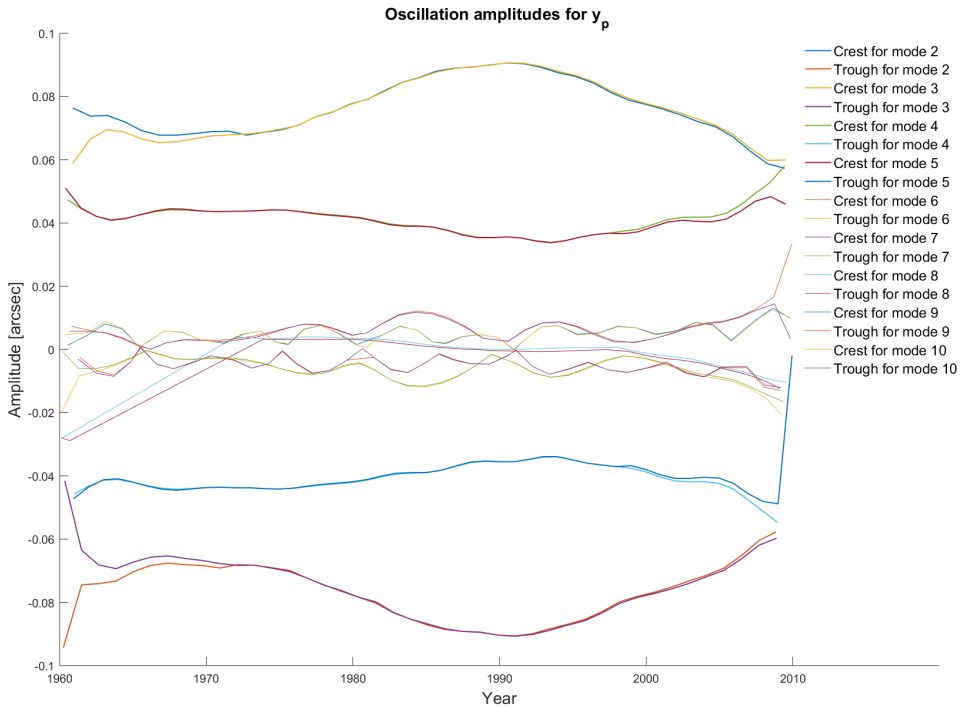

FIGURE 3.5: y_p amplitudes on MSSA reconstructed modes

As shown in the figure.3.5, reconstructed mode 2, mode 3, mode 4 and mode 5 represent main oscillatory components. In order to get the amplitude and frequency for these oscillations, we use the same curve fitting method as chapter.2. The fitting parameters is as following:

TABLE 3.3: Oscillatory modes' fitting parameters for y_{p} by MSSA

fitting parameter	a_1 $[arcsec]$	b_1 $[rad/year]$	c_1 $[rad]$
mode 2	0.076 52	5.306	-47.23
mode 3	0.074 39	5.304	-43.09
mode 4	0.0419	6.293	-8.369
mode 5	0.040 24	6.286	5.931

1. The first reconstructed mode according to the biggest singular value is semi-linear. It is easy to differ mode 1 from the other modes so it is seen as one main component for trend. Reconstructed mode 8 is also like a trend, but the amplitude is too small to take into account.

2. The following four reconstructed modes represent the main oscillatory components of y_{p} time series. The amplitude curve in figure.3.5 of reconstructed mode 2 and mode 3 for y_{p} looks quite similar. So as mode 4 and mode 5. Fitting amplitude for

mode 2 is $0.076\,52$ $[arcsec]$ and the frequency is 5.306 $[arcsec]$. For mode 3 is $0.074\,39$ $[arcsec]$ and 5.304 $[rad/year]$. For mode 4 is 0.0419 $[arcsec]$ and 6.293 $[arcsec]$ and is $0.040\,24$ $[arcsec]$ and 6.286 $[arcsec]$ for mode 5. Selecting the modes with similar amplitudes and frequencies, so we group reconstructed mode 2 with mode 3 into one component and mode 4 and mode 5 into another reconstruction component.

3. For y_{p} reconstructed mode 6, it is not trend but oscillation. The amplitude is obviously close to 0 and the period is not recognized. So it is neither periodic time series nor trend. As for the Polar motion time series analysis, it is not meaningful to study on these small amplitudes' reconstructions. So as the left reconstructed modes. So we just regard all the other modes without mode 1 to mode 5 as residual.

Separation main components of y_{p} by grouping

With decomposition modes for y_{p} shown below, we reconstruct mode 2 and mode 3 as CW, mode 4 and mode 5 as AW, other modes as residual. Reconstructed mode 1 is seen as trend. The main components are shown as :

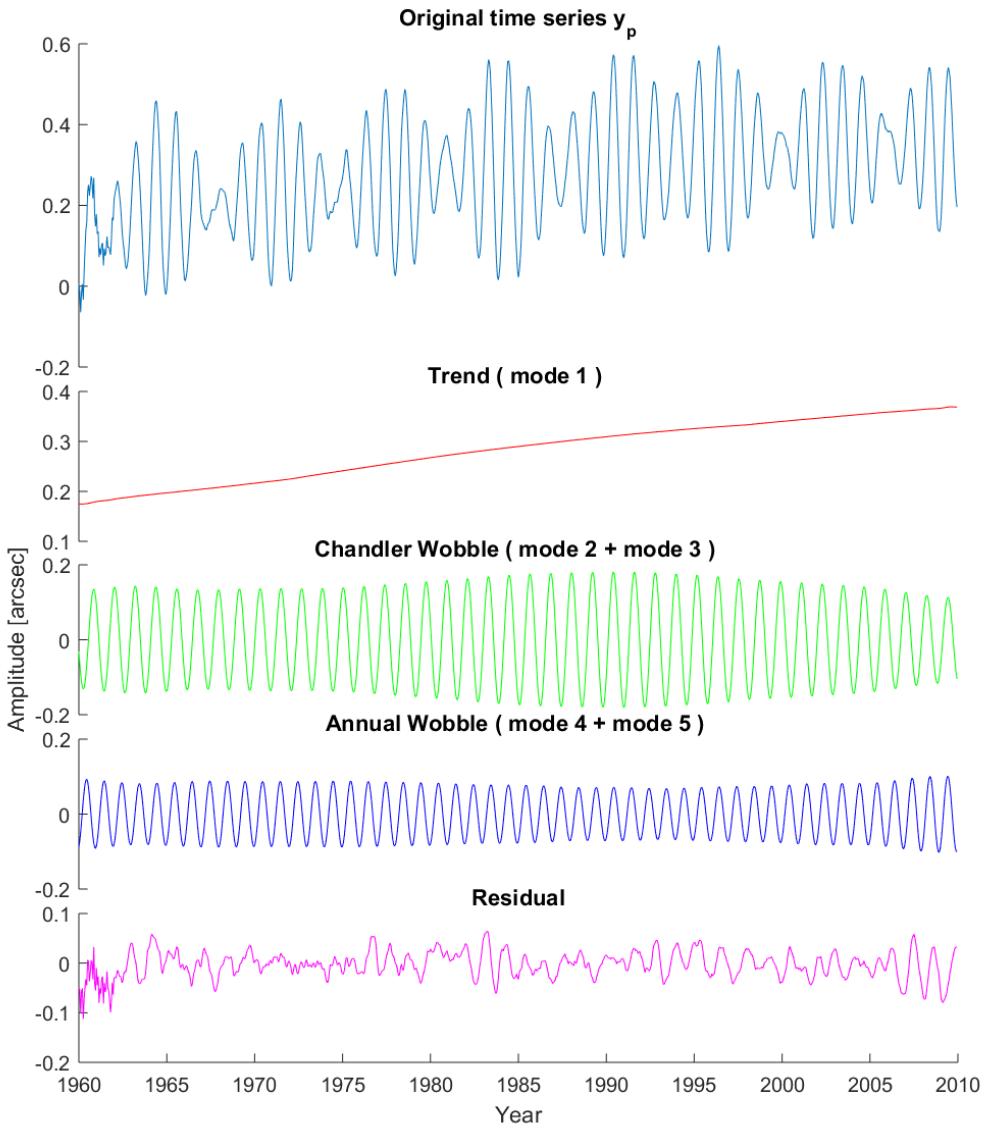

FIGURE 3.6: Main reconstructed components for y_{p} by MSSA

CW and AW are reconstructed by grouping modes together. Apply curve fitting method to get the fitting amplitude and frequency. Fitting parameters are shown as following:

1. Figure.15 shows the original Polar motion time series in the first sub-figure . Then it is trend of y_{p} reconstructed mode 5 which is semi-linear and non-periodic.

TABLE 3.4: Reconstructed components' fitting parameters for y_{p} by MSSA

fitting parameter	a_1 $[arcsec]$	b_1 $[rad/year]$	c_1 $[rad]$
CW	0.1509	5.305	-45.21
AW	$0.082\,02$	6.29	-1.574

2. Grouping y_{p} reconstructed mode 2 and mode 3 as CW. It is shown in the third sub-figure below. Reconstructed CW was fitted by sine function with amplitude of 0.1509 $[arcsec]$ and frequency of 5.305 $[rad/year]$. Then the period calculated by the frequency with the equation.2 is 432.5389. As explained in 1, the period of CW is about 435 days (Höpfner, 2003). Fitting period is almost the same as the research period of CW, so reconstruction of CW for y_{p} by MSSA is believable.

3. Besides, grouping y_{p} reconstructed mode 3 and mode 4 as AW. It is shown in the fourth sub-figure. Its amplitude is around $0.082\,02$ $[arcsec]$ and frequency is about 6.29 $[rad/year]$. So we get the approximate period of AW is 0.9989 $[year]$. With the pre-knowledge, the period of AW is 1 $[year]$ and the amplitude is 0.1 $[arcsec]$ (Höpfner, 2003). The reconstructed amplitude and period are close to the reality. so AW reconstruction for y_{p} by MSSA is in a good result.

4. Residual of y_{p} is shown at last. It is the sum of the other reconstructed modes without the first 5 mode. They are not periodic time series or a trend and their amplitude is smaller than 0.02 $[arcsec]$. So we see them as residual for y_{p}.

Chapter 4

Complex Singular Spectrum Analysis

Complex singular Spectrum Analysis (CSSA) is natural extension of SSA in chapter.2 arises from its expansion to two dimensions with complex value. This chapter gives background for CSSA (Section 4.1), the basic algorithms for CSSA (Section 4.2), as well as the analyzing bivariate time series by combinations $x_{\mathrm{p}} + iy_{\mathrm{p}}$ in Section 4.3 and $y_{\mathrm{p}} + ix_{\mathrm{p}}$ in Section 4.4. At last compare the results from these two kinds of combinations (Section 4.5).

4.1 Background

we can consider one dimensional complex-valued series and apply the complex version of SSA to this one-dimensional series. Complex Singular Spectrum Analysis (CSSA) is a a significant improvement from its expansion to two dimensions of SSA with complex value. It combines bivariate time series together by complex value into one time series. The main algorithm is the same as SSA. CSSA technique expand the SSA technique to the bivariate domain by complex adding.

CSSA uses bivariate time domain data to extract information from short and noisy multivariate time series without prior knowledge of the dynamics affecting the time series. It combines bivariate dimensional data into one dimensional by complex value which is a really novel idea.

Complex values has been used in reconstruction of CW and AW by Fourier basis pursuit band pass filter with combination x_{p} and y_{p} (Wang et al., 2016). CSSA has been applied to large-scale atmospheric fields for forecasting (Mo, 2001). This thesis tries to use CSSA in geodetic time series analysis.

4.2 Methodology

CSSA is a method decomposing the original time series into a sum of independent and interpretable components such as a trend, periodic or quasi-periodic components and noise in two direction at the same time. A brief discussion on the methodology of the CSSA technique is shown as following:

4.2.1 Generation

$Y^1 = \left(x_1^1, x_2^1, x_3^1, \cdots, x_N^1\right)$ and $Y^2 = \left(x_1^2, x_2^2, x_3^2, \cdots, x_N^2\right)$ are real-valued time series with length of N. Firstly generate the new time series as $Y = Y^1 + iY^2 = (x_1, x_2, x_3, \cdots, x_N)$.

4.2.2 Decomposition

We decompose the time series within two steps. The first step is embedding time series Y with lagged vector X_i into the trajectory matrix $\mathbf{X}$. The second step singular value decomposition represents trajectory matrix $\mathbf{X}$ as a sum of bi-orthogonal elementary matrices $\mathbf{X}_i$.

4.2.3 Reconstruction

There are two separate steps: grouping and anti-diagonal averaging. We reconstruct the original time series by grouping to make subgroups of the decomposed trajectory matrix and anti-diagonal averaging to reconstruct the new time series from the subgroups. All the decomposition and reconstruction algorithms for CSSA are the same as SSA.

4.2.4 Separation

Fourthly, since the general algorithm is written down in real valued form, there is the difference in the form of the SVD performed in the complex-valued space, where the transposition should be Hermitian. The initial time series $\mathbf{y}^1 = \left(y_1^1, y_2^1, y_3^1, \cdots, y_N^1\right)$ and $\mathbf{y}^2 = \left(y_1^2, y_2^2, y_3^2, \cdots, y_N^2\right)$ can be reconstructed by

$$y_n^1 = \text{real}(\sum_{i=1}^{m} z_n^{(i)}(n = 1, 2, \cdots, N)), \tag{4.1}$$

and

$$y_n^2 = -\text{imag}(\sum_{i=1}^{m} z_n^{(i)}(n = 1, 2, \cdots, N)). \tag{4.2}$$

4.3 CSSA of time series $x_{\mathrm{p}} + iy_{\mathrm{p}}$

Organize the new time series generating polar motion time series x_{p} in the time period spanning from 1960 to 2009 for the real part and y_{p} for the imaginary part. Apply CSSA on the organized time series with the window length of $L = 240$. Then we get decomposition for x_{p} based on the real part and y_{p} in the imaginary part of separating main components as trend, Chandler wobble, annual wobble and residual.

4.3.1 Separation of real part x_{p}

Apply CSSA on the new organized complex time series and select the real part of decomposition as x_{p} time series. We analyze the first 10 modes for real part and separate main components for it. The plot for the mode 1 to mode 10 is as following:

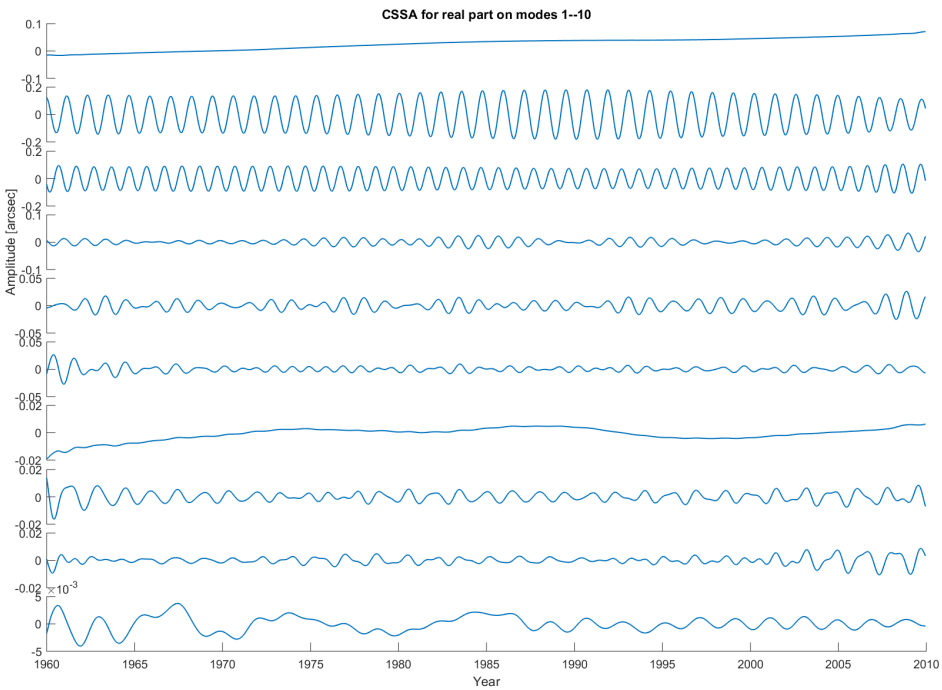

FIGURE 4.1: Reconstructed modes 1–10 of the time series real part by CSSA

In order to separate modes into different components, we plot x_{p} amplitudes of oscillatory modes shows as following:

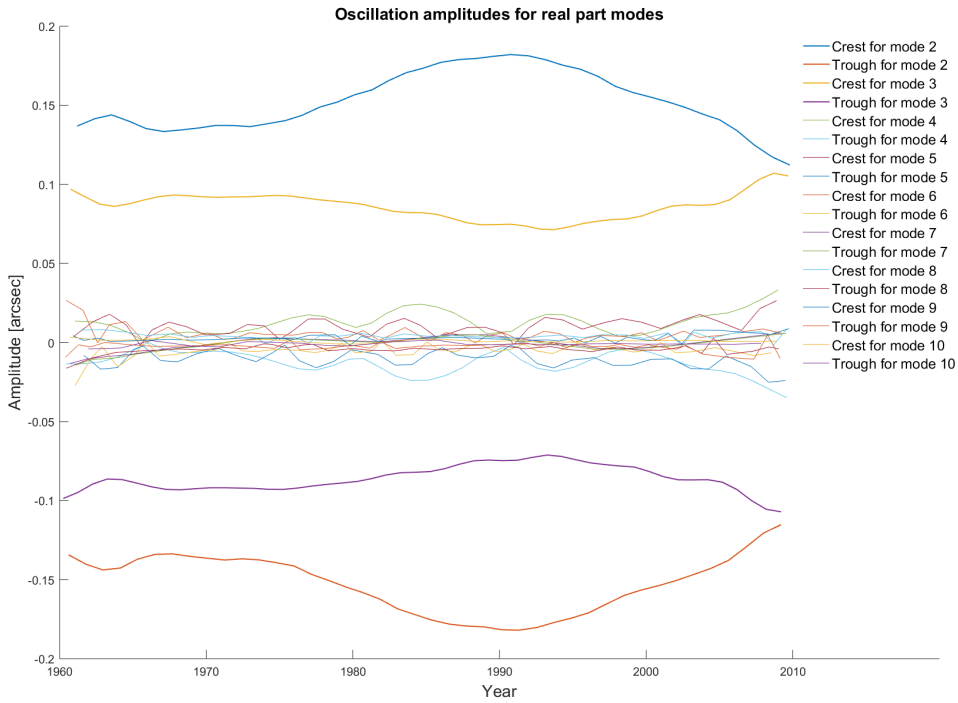

FIGURE 4.2: Real part amplitudes on CSSA reconstructed modes

1. It is obvious to see that real part for the first reconstructed mode represents trend. It is quite different from other modes which are oscillatory reconstructions of x_{p} time series.

2. The real part for second mode is oscillatory reconstruction. As shown in figure.4.2, the amplitude is the strongest near by 0.15 $[arcsec]$. So the real part for second reconstructed mode is seen as CW for x_{p}.

3. Real part reconstructed mode 3 is also oscillatory component but with smaller amplitude compared with mode 2. The amplitude is near by 0.1 $[arcsec]$. As a result, real part of reconstructed mode 3 is considered as AW for x_{p}.

4. Reconstructed mode 4 for real part is also oscillation. But the amplitude is obviously smaller than the mode 2 and mode 3 and the period is not easily recognized. So it is neither periodic time series nor trend. So as the other modes. The amplitude is smaller than 0.04 $[arcsec]$, So we just regard all the left modes as residual for x_{p}.

Reconstructed mode 1 for is seen as trend, mode 2 as CW, mode 3 as AW, other modes as residual. Main components are shown as:

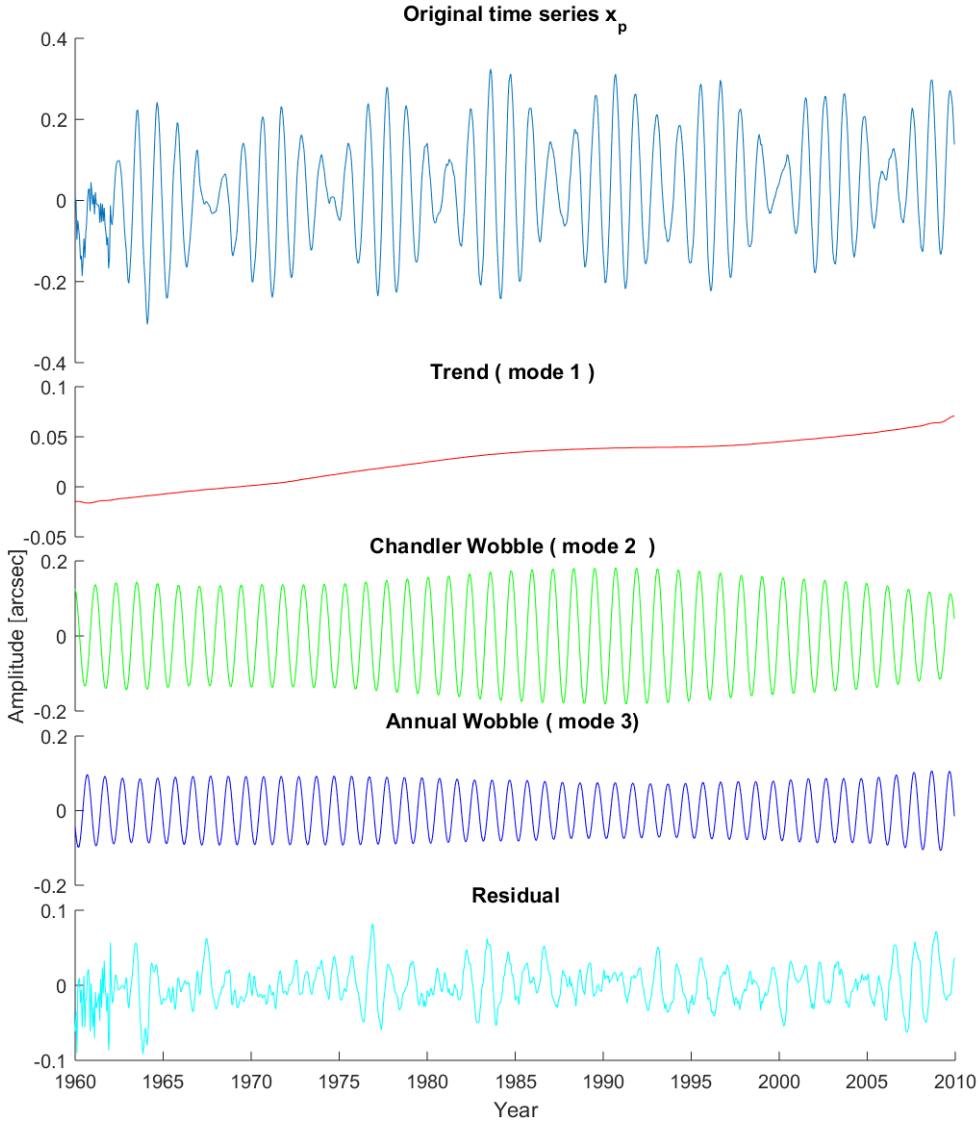

FIGURE 4.3: Main components for x_{p} by CSSA in real part

In oder to analyze CW and AW, we use the curve fitting method to get fitting amplitude and frequency.

TABLE 4.1: Reconstructed components' fitting parameters for x_{p} by CSSA

fitting parameter	a_1 [arcsec]	b_1 $[rad/year]$	c_1 $[rad]$
CW	0.1517	5.305	-40.88
AW	$0.086\,38$	6.289	-2.565

1. The first sub-figure of figure.4.3 shows the original polar motion time series in x direction x_{p}. The second one from reconstructed mode 1 of x_{p} is trend by CSSA.

2. Reconstructed mode 2 in the real part is seen as CW for x_{p} and it is shown in the third sub-figure below. The fitting frequency of reconstructed CW for x_{p} is 5.305 $[rad/year]$. Calculating by equation: $T = \dfrac{2\pi}{f}$, the period reconstructed CW is 432.5389 days. As explained polar motion time series in chapter.1, the period of CW is about 435 days (Höpfner, 2003). The result we get is similar to the period of CW, so the reconstruction of the CW for x_{p} by CSSA in the real part is credible.

3. Reconstructed mode 3 in the real part is shown in the fourth sub-figure. It is seen as the AW for x_{p}. Its amplitude by fitting is $0.086\,38$ $[arcsec]$ and period calculated by equation2 is 0.999 $[year]$. As we know, the period of AW is 1 year and the amplitude is 0.1 $[arcsec]$ (Höpfner, 2003). So CSSA is a good method for separating the AW from the real part from new reconstructed time series.

4. Residual of x_{p} is shown in the last one. It is the sum of the left reconstructed modes in the real part whose amplitude is smaller than 0.02 $[arcsec]$.

4.3.2 Separation of imaginary part y_{p}

Apply CSSA on the new organized complex time series and select the imaginary part of decomposition as y_{p} time series. Then plot the first 10 modes and separate the main components for y_{p}. The plot for the mode 1 to mode 10 is as following:

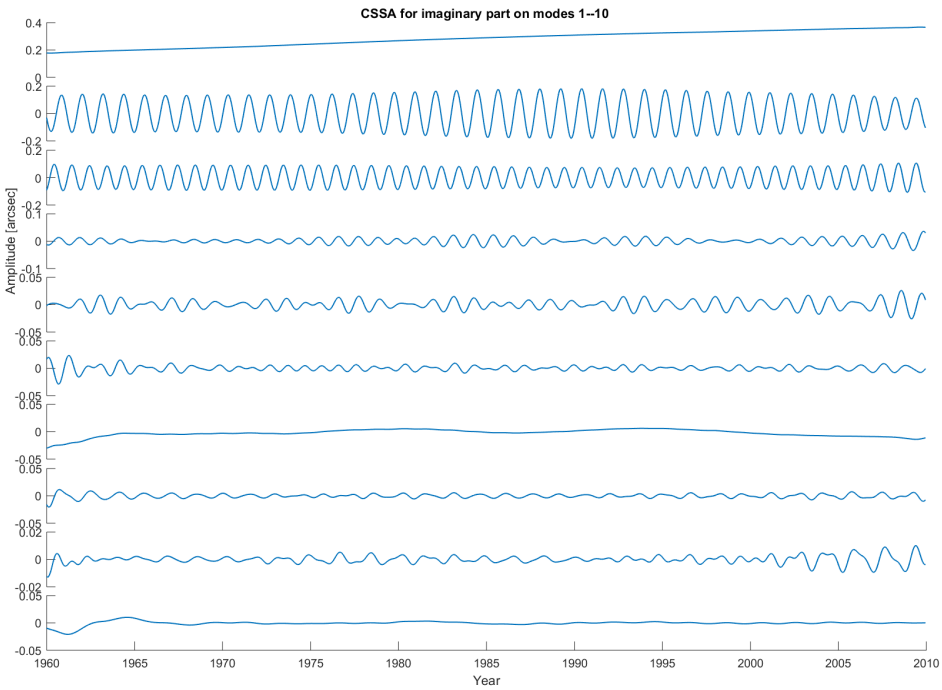

FIGURE 4.4: Reconstructed modes 1–10 of the time series imaginary part by CSSA

In order to separate the modes into different components by amplitude, y_{p} amplitudes of oscillatory modes shows as following:

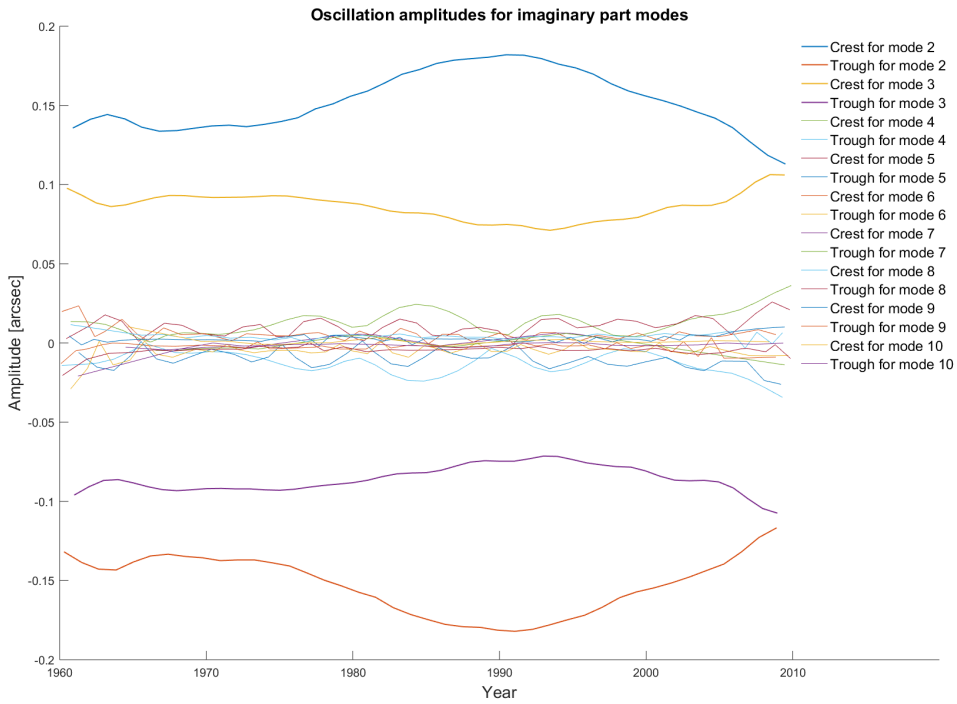

FIGURE 4.5: Imaginary part amplitudes on CSSA reconstructed modes

1. As shown in figure.4.4, it is obvious to see that the first reconstructed mode for the imaginary part is trend which is quite different from other modes. Others are oscillatory reconstructions for the imaginary part of time series.

2. The second reconstructed mode for the imaginary part is an oscillation. As shown in 4.5, the amplitude for mode 2 is the strongest from 0.12 to 0.18 $[arcsec]$. So it is recognized as CW for y_{p}.

3. Reconstructed mode 3 for y_{p} is also oscillatory component but with smaller amplitude compared with mode 2. The amplitude is close to 0.1 $[arcsec]$. So we consider reconstructed mode 3 in the imaginary part as AW for y_{p}.

4. The left reconstructed modes for the imaginary part are also oscillations. But amplitudes of them is smaller than 0.04 $[arcsec]$ and the period is not easily recognized. So it is neither periodic time series nor trend. So we just regard all the left modes as residual for y_{p}.

Reconstructed mode 1 in the imaginary part is seen as trend for y_{p}, mode 2 as CW, mode 3 as AW, sum of other modes as residual. Main reconstructed components are shown as following:

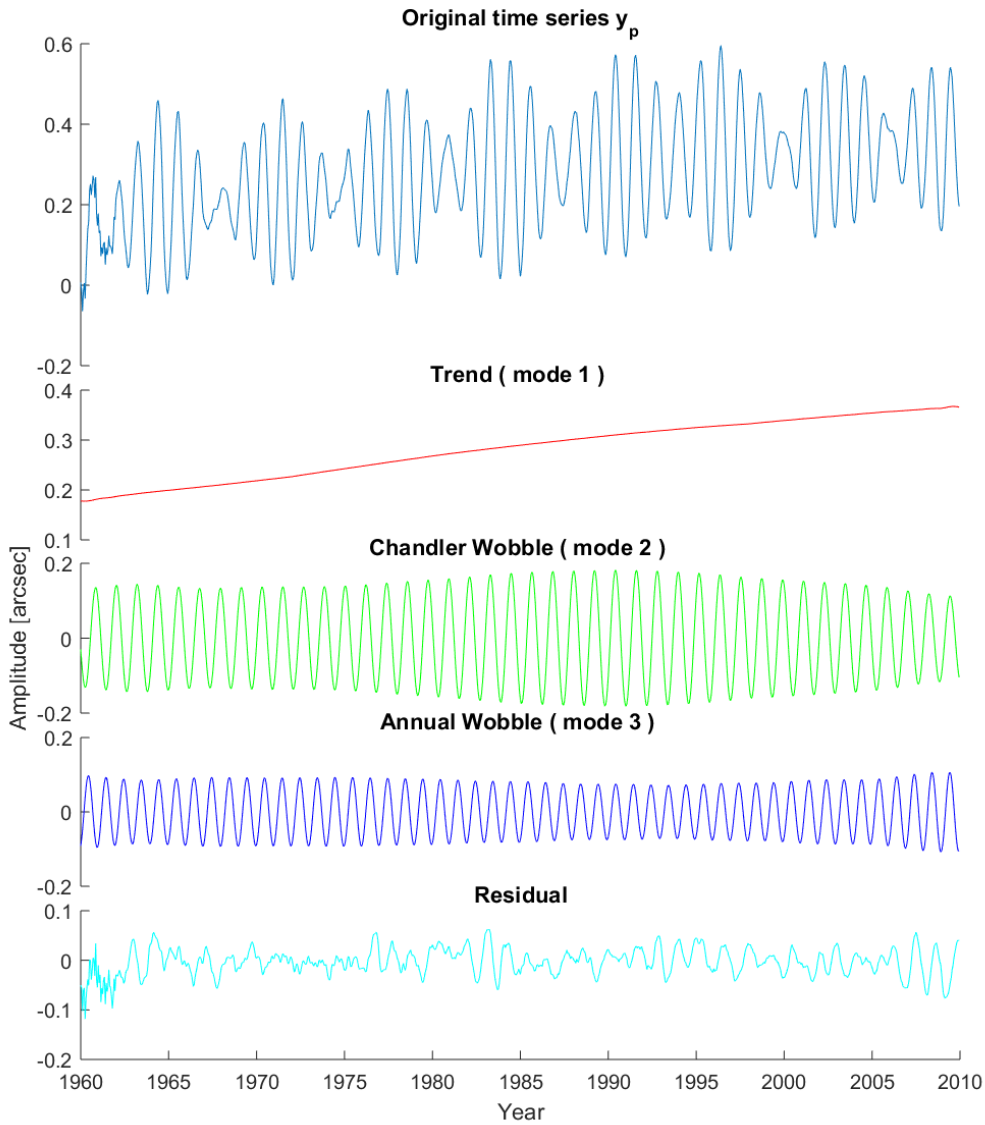

FIGURE 4.6: Main components for y_p by CSSA in imaginary part

In oder to analyze the new reconstructed components, we get fitting amplitude and frequency by 'cftool' in Matlab. The fitting parameters is as following:

TABLE 4.2: Reconstructed components' fitting parameters for y_{p} by CSSA

fitting parameter	a_1 $[arcsec]$	b_1 $[rad/year]$	c_1 $[rad]$
CW	0.1515	5.305	-45.42
AW	$0.086\,35$	6.29	-1.281

1. Original polar motion time series in y direction y_{p} shows in the first sub-figure of figure.4.6. The second one is trend from reconstructed mode 1 in the imaginary part for y_{p} by CSSA.

2. Reconstructed mode 2 shown in the third sub-figure below is seen as CW for y_{p}. The fitting frequency of CW reconstructed by CSSA for y_{p} is 5.305 $[rad/year]$. With equation $T = \frac{2\pi}{f}$, we calculate the period of CW and get the result of 432.5389 days. The period of CW in polar motion time series explained in 1 is about 435 days (Höpfner, 2003). Fitting period of CW reconstructed by CSSA is almost the same to the period of CW, so CSSA is a good choice to reconstruct CW.

3. Reconstructed mode 3 in the imaginary part is shown in the fourth sub-figure. It is seen as the AW for y_{p}. Its fitting amplitude is $0.086\,35$ $[arcsec]$ and period calculated by equation.2 with fitting frequency of 6.29 $[rad/year]$ is 0.9989 $[year]$. As we know, the period of AW is 1 year and the amplitude is 0.1 $[arcsec]$ (Höpfner, 2003). So CSSA is also a method for separating the AW from imaginary part of the new reconstructed time series.

4. The last one is residual for y_{p}. It is the sum of the left reconstructed modes in the imaginary part whose amplitude is smaller than 0.04 $[arcsec]$.

4.4 CSSA of time series $y_{\mathrm{p}} + ix_{\mathrm{p}}$

Organize a new Polar motion time series in y direction y_{p} for the real part and in x direction x_{p} for the imaginary part. Apply CSSA on the organized time series with the window length of $L = 240$. Then we get decomposition for y_p based on the real part and x_{p} in the imaginary part of the analysis result to separate main components of the new polar motion time series for trend, Chandler wobble, annual wobble and residual.

4.4.1 Separation of imaginary part x_{p}

Apply CSSA on the new organized complex time series and select imaginary part of decomposition as x_{p} time series. We select the first 10 modes to analyze and separate the main components for x_{p}. The plot for the mode 1 to mode 10 is as following:

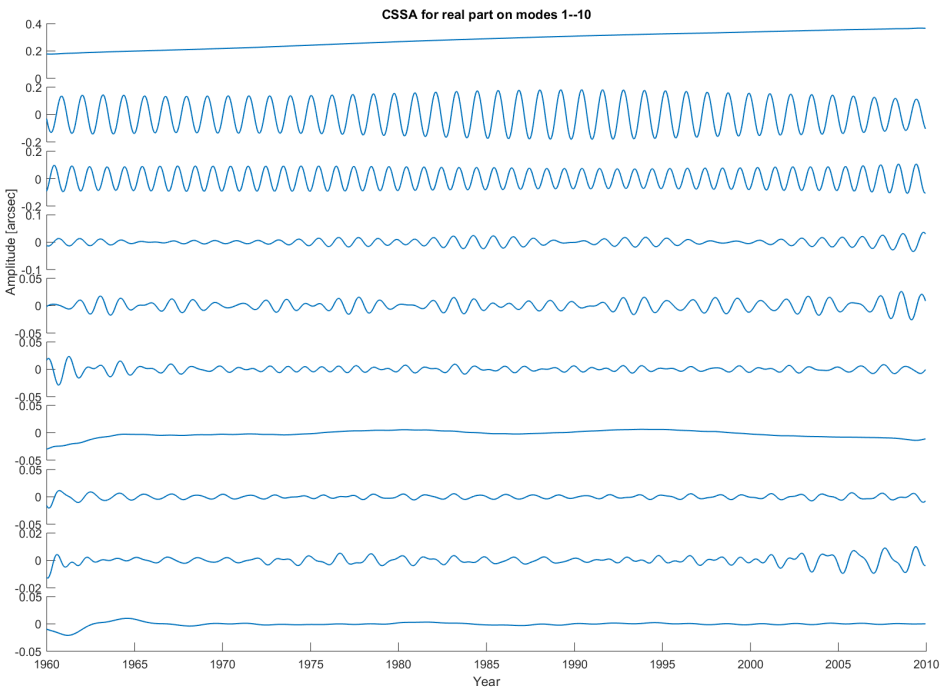

FIGURE 4.7: Reconstructed modes 1–10 of imaginary part by CSSA

In order to separate the modes into different components, amplitudes of oscillatory modes of imaginary part for x_p shows as following:

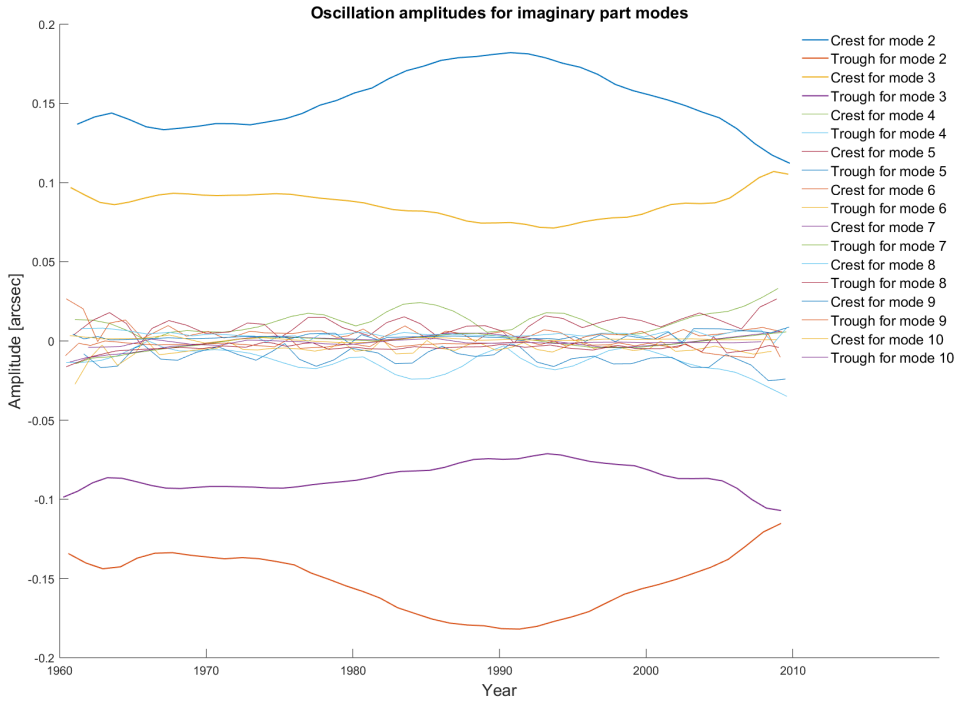

FIGURE 4.8: Imaginary part amplitudes on CSSA reconstructed modes

1. Imaginary part of decomposition result is x_{p}. So we see that the first reconstructed mode represents trend for x_{p}. It is quite different from other modes which are oscillatory reconstructions.

2. Reconstructed mode 2 for imaginary part is an oscillatory reconstruction. As shown in figure.4.8, the amplitude is the strongest which is near 0.1517 $[arcsec]$. So the second reconstructed mode is seen as one main component CW for x_{p}.

3. Reconstructed mode 3 for imaginary part is also an oscillatory component but with smaller amplitude compared with mode 2. The amplitude is near 0.08638 $[arcsec]$. As a result, reconstructed mode 3 is considered as another main component for x_{p}.

4. Reconstructed mode 4 is for imaginary part also an oscillation. But the amplitude is obviously smaller than the mode 2 and mode 3 and the period is not easily recognized. So it is neither periodic time series nor trend. The other modes also with amplitude which is smaller than 0.04 $[arcsec]$, So we just regard all the left modes as residual.

we generate main components for imaginary part x_{p} are shown as following:

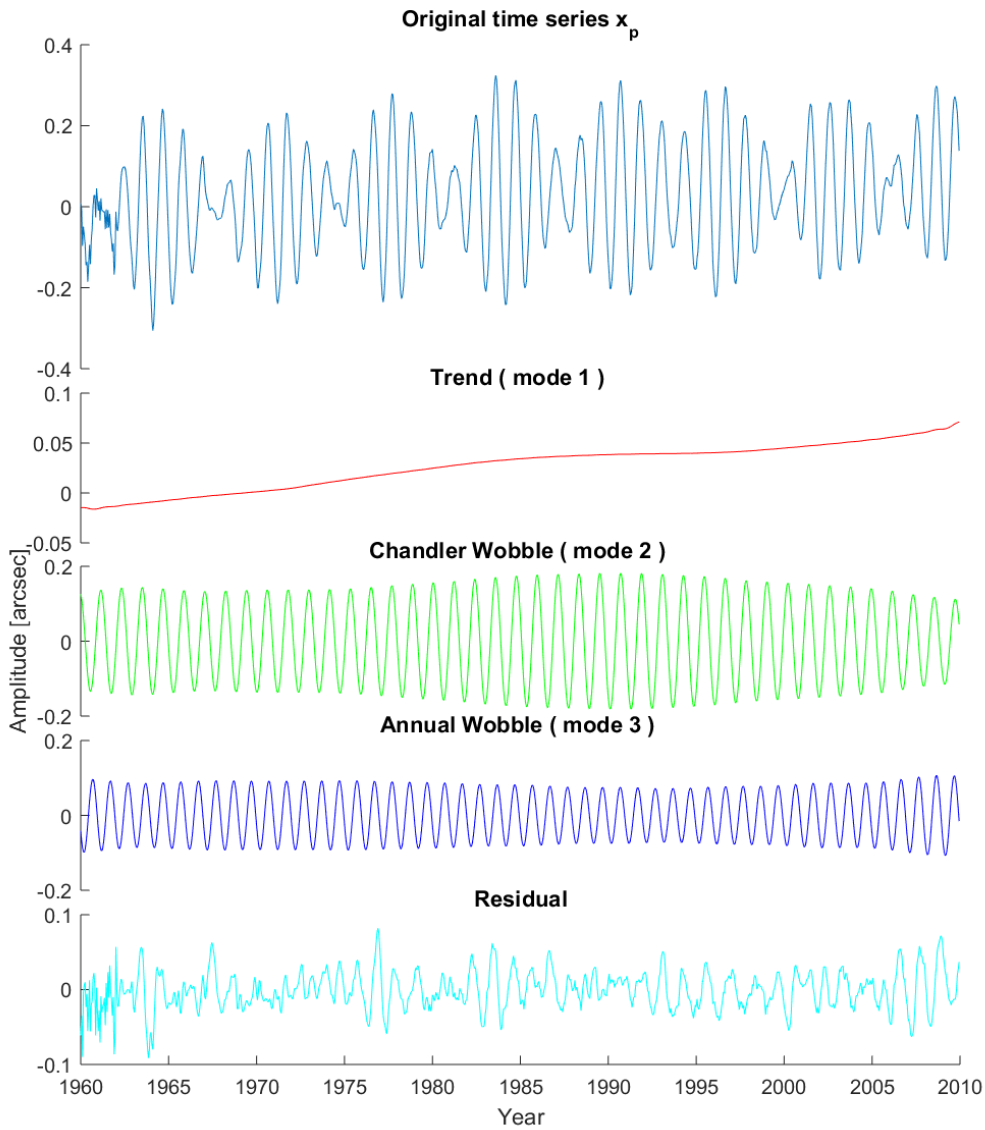

FIGURE 4.9: Main components for x_{p} by CSSA in imaginary part

In oder to analyze CW and AW, we use the curve fitting method to get fitting amplitude and frequency.

TABLE 4.3: Reconstructed components' fitting parameters for x_{p} by CSSA

fitting parameter	a_1 $[arcsec]$	b_1 $[rad/year]$	c_1 $[rad]$
CW	0.1517	5.305	-40.88
AW	$0.086\,38$	6.289	-2.565

1. Original polar motion time series in x direction x_{p} shows in the first sub-figure of figure.4.9. The second one from reconstructed mode 1 according to the imaginary part of new reconstructed time series is trend by CSSA.

2. Reconstructed mode 2 in the imaginary part is seen as CW and it is shown in the third sub-figure below. The fitting frequency of CW for x_{p} is 5.305 $[rad/year]$. Use the equation $T = \dfrac{2\pi}{f}$ to calculate period of CW. So we get the period of CW for 432.5389 days. As explained in chapter.1, the period of CW is about 435 days (Höpfner, 2003). The period for reconstructed CW by CSSA is near to the real period. So CSSA is a method to separate CW from polar motion time series in the imaginary part.

3. Reconstructed mode 3 in the imaginary part is shown in the fourth sub-figure. It is seen as the AW for x_{p}. Its amplitude by fitting is $0.086\,38$ $[arcsec]$ and period calculated by equation2 is 0.999 $[year]$. As the period of AW is 1 year and the amplitude is 0.1 $[arcsec]$ (Höpfner, 2003). So CSSA is a choice for separating the AW from the complex polar motion time series.

4. Residual for x_p is shown in the last one. It is the sum of the left reconstructed modes in the imaginary part whose amplitude is smaller than 0.02 $[arcsec]$.

4.4.2 Separation of real part y_{p}

Apply CSSA on the new organized complex time series and select the real part as decomposition for y_{p} time series. We analyze the first 10 modes in the the real part and separate the main components for it. The plot for the mode 1 to mode 10 is as following:

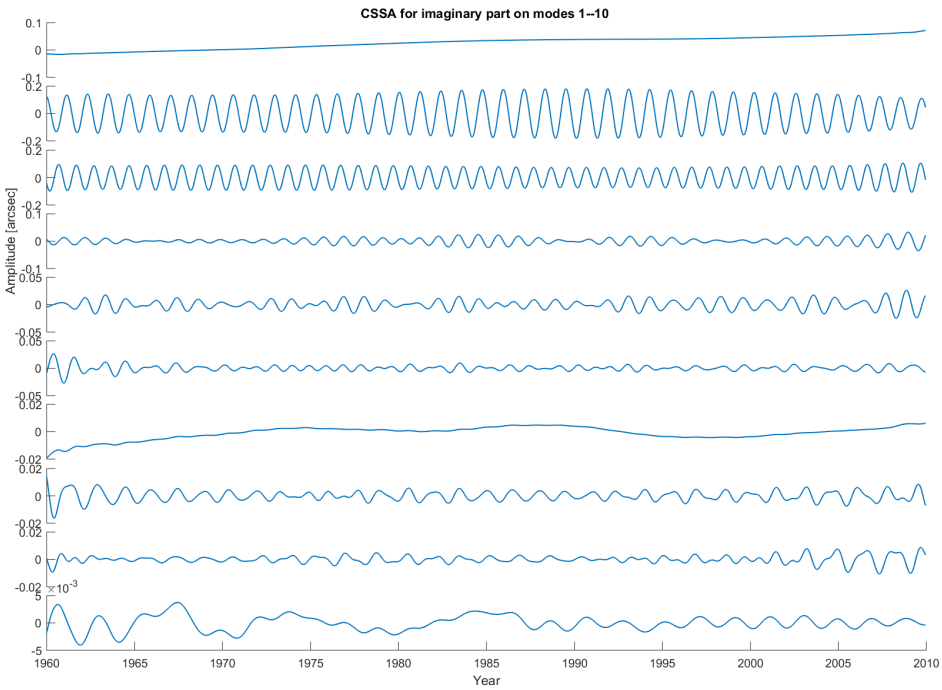

FIGURE 4.10: Reconstructed modes 1–10 of real part by CSSA

In order to separate the modes into different components, amplitudes of oscillatory modes in real part shows as following:

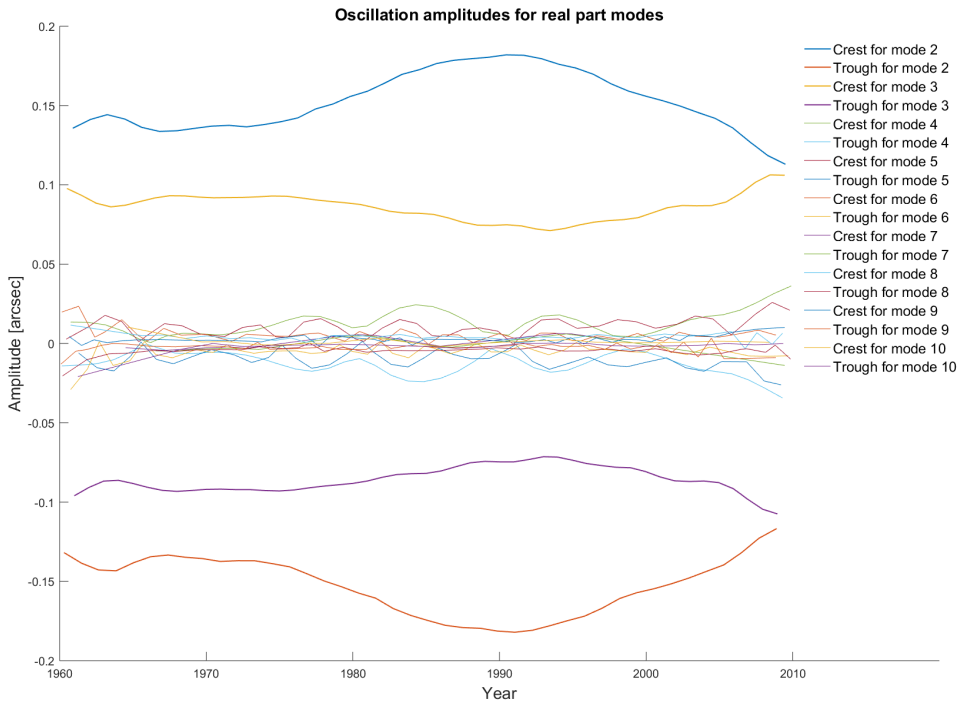

FIGURE 4.11: Real part amplitudes on CSSA reconstructed modes

1. It is obvious to see that the first reconstructed mode in the real part represents trend for y_{p}. It is quite different from other modes which are oscillatory reconstructions in the real part.

2. The second reconstructed mode is an oscillatory reconstruction. As shown in figure.4.11, the amplitude is the strongest from 0.1 $[arcsec]$ to 0.2 $[arcsec]$. So the second reconstructed mode is seen as CW for y_{p}.

3. Reconstructed mode 3 in the real part is also oscillatory component but with smaller amplitude compared with mode 2. The amplitude is from 0.07 $[arcsec]$ to 0.12 $[arcsec]$. As a result, reconstructed mode 3 in the real part is considered as AW for y_{p}.

4. Reconstructed mode 4 for y_{p} is also oscillation. But the amplitude is obviously smaller than the mode 2 and mode 3 and the period is not recognizable. So it is neither periodic time series nor trend. So as the other modes with amplitudes smaller than 0.05 $[arcsec]$. So we just regard all the left modes in the real part as residual

for y_{p}.

Reconstructed mode 1 in the real part for y_{p} is seen as trend, mode 2 as CW, mode 3 as AW, other modes as residual. Main components for y_{p} are shown as:

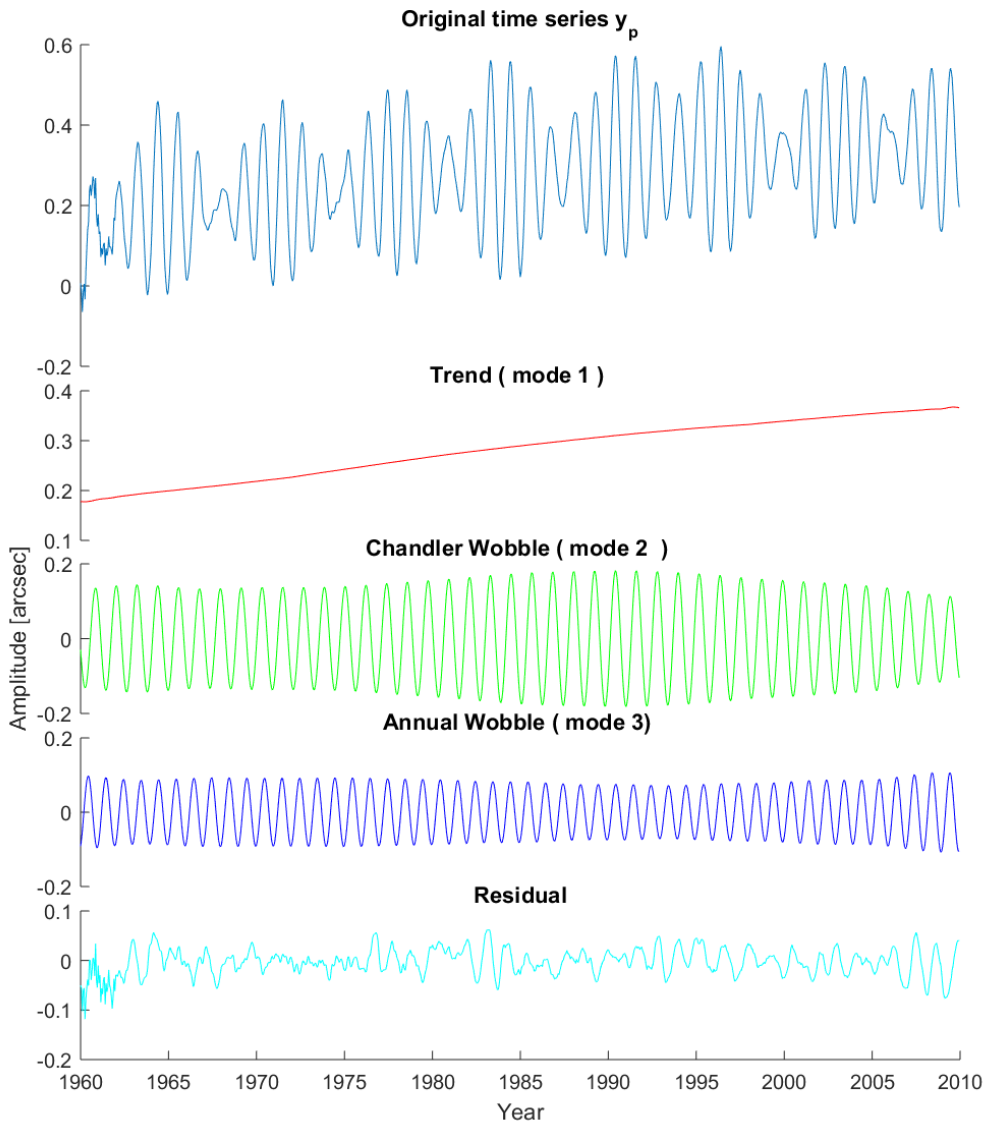

FIGURE 4.12: Main components for y_{p} by CSSA in real part

In oder to analyze CW and AW, we use the curve fitting method to get fitting amplitude and frequency.

TABLE 4.4: Reconstructed components' fitting parameters for y_{p} by CSSA

fitting parameter	a_1 $[arcsec]$	b_1 $[rad/year]$	c_1 $[rad]$
CW	0.1525	5.305	-45.42
AW	$0.086\,35$	6.29	-1.281

1. The first sub-figure of figure.4.12 shows the original Polar motion time series in y direction y_{p}. The second sub-figure reconstructed from mode 1 in the real part is trend for y_{p} by CSSA.

2. Reconstructed mode 2 is seen as CW for y_{p} and it is shown in the third sub-figure below. The fitting frequency of reconstructed CW for y_{p} is 5.305 $[rad/year]$. Calculate the period by the equation: $T = \dfrac{2\pi}{f}$, we get period of CW is 432.5389 days. As explained in 1 for polar motion time series, the period of CW is about 435 days (Höpfner, 2003). It is similar to the period of CW, so the CW reconstruction by CSSA by separating real part is credible.

3. Reconstructed mode 3 in the real part is shown in the fourth sub-figure. It is seen as AW for y_p. Its amplitude by fitting is $0.086\,35$ $[arcsec]$ and period calculated with fitting frequency is 0.9989 $[year]$. As we know, the period of AW is 1 year and the amplitude is 0.1 $[arcsec]$ (Höpfner, 2003). So CSSA is a method for AW reconstruction from y_p in the real part.

4. Residual of y_{p} is shown in the last sub-figure. It is the sum of the left reconstructed modes whose amplitude is smaller than 0.05 $[arcsec]$ in the real part.

4.5 Comparison CSSA on $x_{\mathrm{p}} + iy_{\mathrm{p}}$ with $y_{\mathrm{p}} + ix_{\mathrm{p}}$

We combine polar motion time series x_{p} and y_{p} in two ways: $x_{\mathrm{p}} + iy_{\mathrm{p}}$ in Section 4.3 and $y_{\mathrm{p}} + ix_{\mathrm{p}}$ in Section 4.4. Then apply CSSA on new organized time series and separate main components from x_{p} and y_{p} as trend, CW, AW and residual. In this section, we will compare the results by these two kinds of combinations.

4.5.1 Comparison of x_p main components

Apply CSSA on the new organized complex time series in two forms on $x_p + iy_p$ and $y_p + ix_p$ and separate x_p into trend, CW and AW. The plot of the main components' differences by the two forms for x_p are as following:

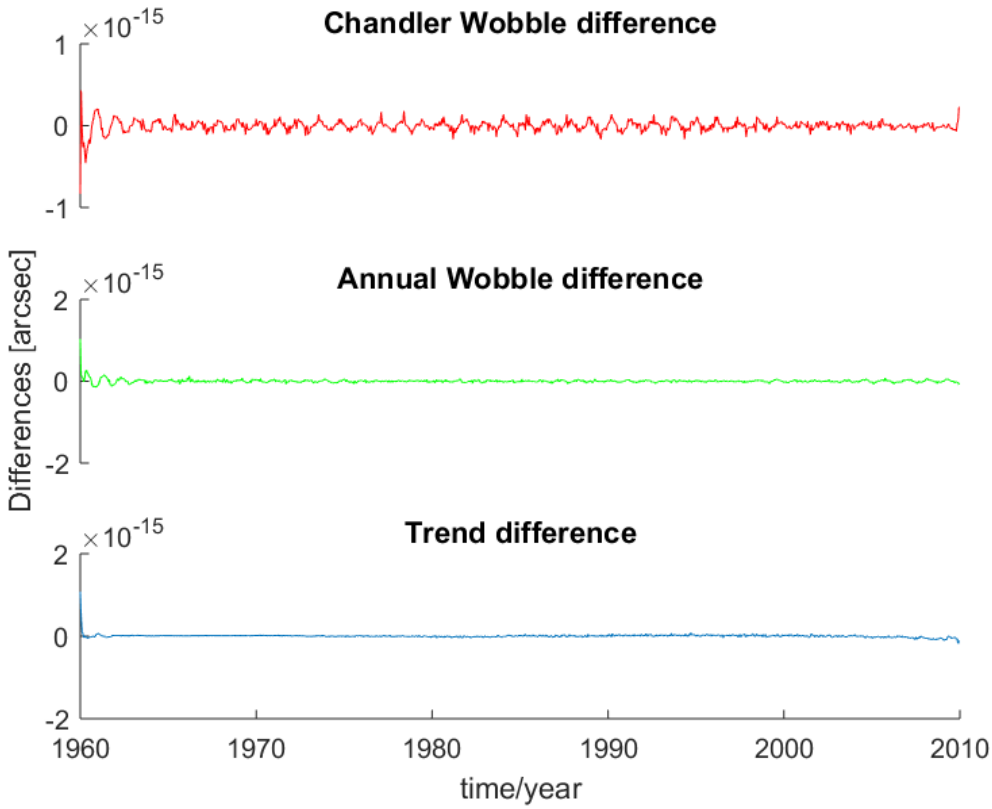

FIGURE 4.13: Differences of main components for x_p

Differences between x_p main components separated by CSSA on the two new reconstructed time series is quite small in the scale of 10^{-15} $[arcsec]$. So we can conclude that it doesn't matter whether x_p in real part or in imaginary part for x_p decomposition.

4.5.2 Comparison of y_{p} main components

Apply CSSA on the new organized complex time series in two forms on $x_{\mathrm{p}} + iy_{\mathrm{p}}$ and $y_{\mathrm{p}} + ix_{\mathrm{p}}$ and separate trend, CW and AW for y_{p}. We compare the decomposition result for the three main components of $x_{\mathrm{p}} + iy_{\mathrm{p}}$ with $y_{\mathrm{p}} + ix_{\mathrm{p}}$. The differences show as following:

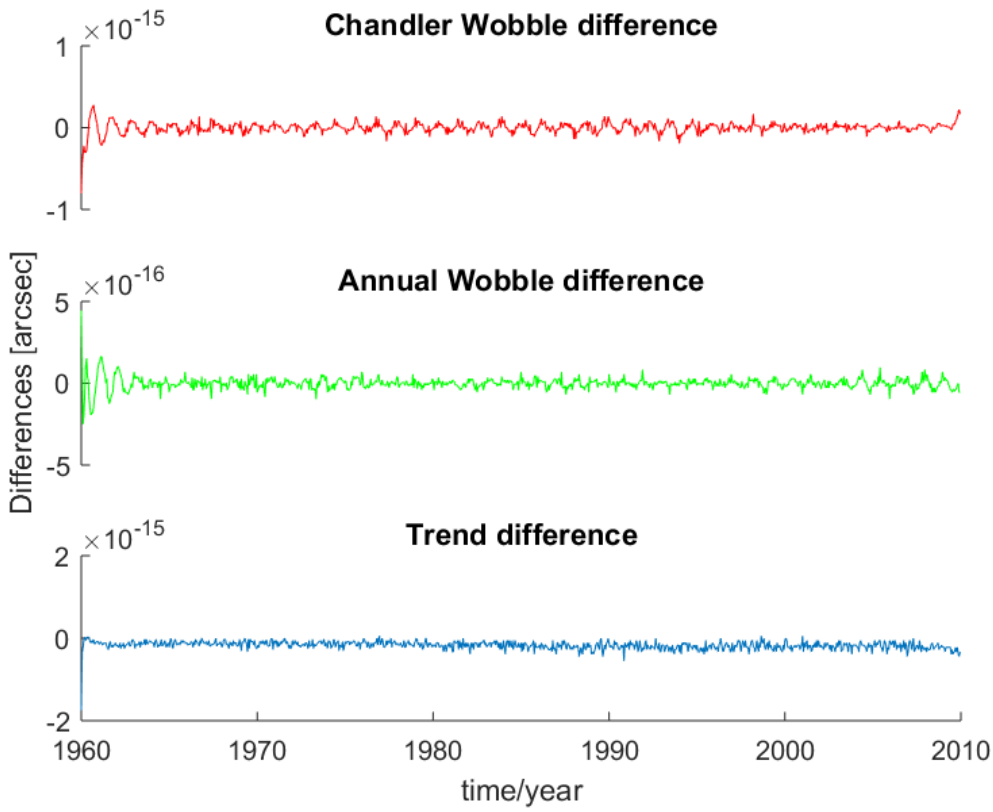

FIGURE 4.14: Differences of main components for y_{p}

It is obvious that differences between main components for y_{p} separated by CSSA on the two new reconstructed time series is quite small. Differences for CW and trend are in the scale of 10^{-15} $[arcsec]$ and 10^{-16} $[arcsec]$ for AW. As a conclusion, it doesn't matter whether y_{p} in real part or in imaginary part for y_{p} decomposition. CSSA In the next chapter, we just choose $x_{\mathrm{p}} + iy_{\mathrm{p}}$ as combination form.

Chapter 5

Summary and outlook

This chapter gives comparison MSSA and CSSA with SSA on decomposing polar motion time series (Section 5.1), conclusion (Section 5.2) as well as outlook (Section 5.3).

5.1 Comparison CSSA with SSA and MSSA

5.1.1 Reconstructed modes comparison

This thesis analyzes polar motion observations in the time period spanning from 1960 to 2009 both in x direction and y direction with three methods: SSA, MSSA and CSSA which are nonparametric spectral estimation methods in time series analysis. They are aids in the decomposition of polar motion time series into a sum of independent and interpretable components as trend, CW, AW and residual. These components are grouped by different modes according to different singular values. Modes in different methods show in the following:

TABLE 5.1: Modes for decomposition main components by different methods

methods	SSA (for x_{p})	SSA (for y_{p})	MSSA (for x_{p})	MSSA (for y_{p})	CSSA (for x_{p} and y_{p})
Trend	mode 5	mode 1	mode 1 and mode 8	mode 1	mode 1
Chandler Wobble	mode 1 and mode 2	mode 2 and mode 3	mode 2 and mode 3	mode 2 and mode 3	mode 2
Annual Wobble	mode 3 and mode 4	mode 4 and mode 5	mode 4 and mode 5	mode 4 and mode 5	mode 3
Residual	else	else	else	else	else

It is easily recognized that there is much difference between different methods for separating main components. For x_{p} trend reconstruction, there is no regular pattern. But for y_{p}, trend is reconstructed by mode 1 for all the three methods which means that trend for y_{p} is more obvious than for x_{p}.

For CW reconstruction, two modes are grouped in SSA and MSSA methods but just one single mode in CSSA. So as AW reconstruction. But the numbers of modes for AW are bigger than CW which means singular values in SVD for AW are smaller than CW.

For SSA on both x_{p} and y_{p}, we combine different modes to reconstruct CW and AW. But just use single mode for trend reconstruction.

For MSSA on both x_{p} and y_{p}, we combine mode 2 and mode 3 to reconstruct CW and mode 4 and mode 5 to AW. But different reconstructed modes for trend reconstruction.

For CSSA on both x_{p} and y_{p}, we just put single mode to reconstruct trend, CW or AW. And reconstructed mode for x_{p} and y_{p} are the same. With respect to SSA and MSSA methods, it shows advantage of CSSA that it can analyze bivariate time series at the same time with just single mode for reconstruction.

5.1.2 Main components comparison

SSA, MSSA and CSSA are methods on decomposition of x_{p} and y_{p} into a sum of trend, CW, AW and residual. But reconstructions are different by using different methods. Consider SSA method as a standard, calculate differences between MSSA and SSA as well as CSSA and SSA.

comparison for x_{p} components

Decomposition of x_{p} are different by using different methods. Amplitude differences between CSSA and SSA and CSSA and MSSA are shown as following:

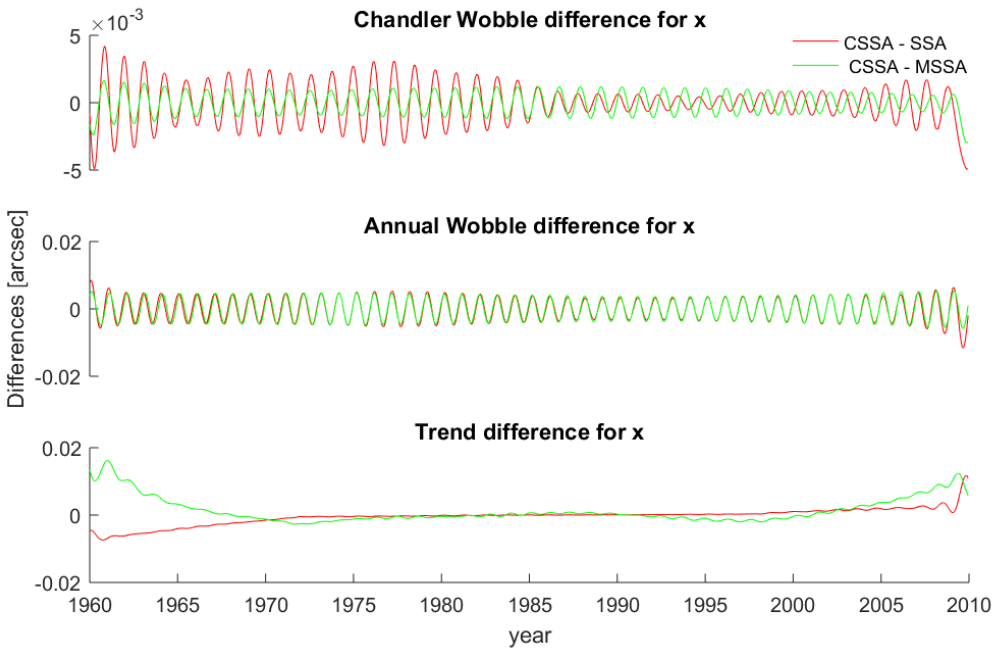

FIGURE 5.1: Differences for x_{p}

In oder to evaluate quality of the differences, we calculate the RMS. RMS for the x_{p} differences shows as following:

TABLE 5.2: RMS for the methods differences for x_{p}

RMS for differences	CW	AW	trend
CSSA-SSA	0.0015	0.0033	0.0024
CSSA-MSSA	$8.0749e-04$	0.0031	0.0040

The difference between CSSA and SSA for x_{p} CW is in 0.0005 $[arcsec]$ with RMS of 0.0015. In addition, difference between CSSA and MSSA for CW is in 0.0005 $[arcsec]$ with the RMS of $8.0749e-04$. With this values, we can conclude that CW reconstruction with CSSA method is in a high quality.

For x_{p} AW reconstruction, difference between CSSA and SSA is in 0.015 $[arcsec]$ with the RMS of 0.0033. And 0.01 $[arcsec]$ with the RMS of 0.0031 between CSSA and MSSA. Although AW reconstruction is not so good as CW reconstruction, CSSA is also a good choice.

For x_{p} trend, difference is in 0.015 $[arcsec]$ with RMS of 0.0024 between CSSA and SSA. And 0.01 $[arcsec]$ with RMS of 0.004 between CSSA and MSSA. So CSSA perform well in reconstruction CW, AW and trend for x_{p}.

comparison for y_{p} components

Decomposition of y_{p} are different by using different methods. Amplitude differences are shown as following:

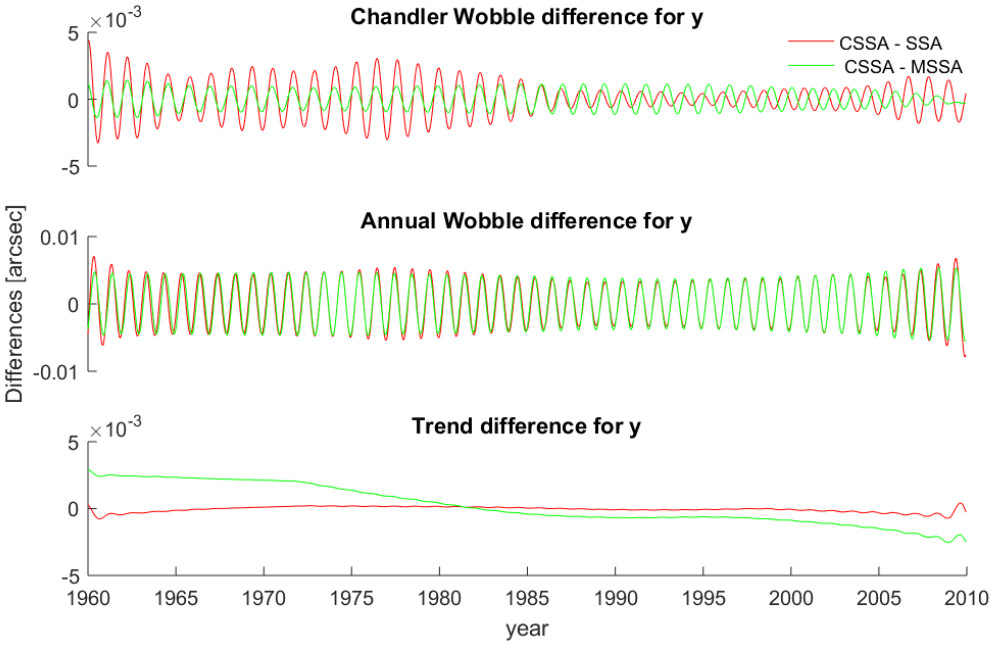

FIGURE 5.2: Differences for y_{p}

RMS for the methods differences for y_{p} shows as following:

TABLE 5.3: RMS for the methods differences for y_{p}

RMS for differences	CW	AW	trend
CSSA-SSA	0.0013	0.0032	$2.1443e-04$
CSSA-MSSA	$7.1005e-04$	0.0031	0.0015

For y_{p} CW reconstruction, the difference between CSSA and SSA is in 0.0005 $[arcsec]$ with RMS of 0.0013. Between CSSA and MSSA for CW is in $7.1005e-04$ $[arcsec]$ with RMS of $7.1005e-04$. The quality for CW reconstruction is satisfied.

For y_{p} AW reconstruction, difference between CSSA and SSA is in 0.01 $[arcsec]$ with RMS of 0.0032. And 0.01 $[arcsec]$ with RMS of 0.0031 between CSSA and MSSA.

For y_{p} trend reconstruction, difference is in 0.0005 $[arcsec]$ with RMS of $2.1443e-04$ between CSSA and SSA. And 0.0005 $[arcsec]$ with RMS of 0.0015 between CSSA and MSSA. It can conclude that CSSA perform well in decomposing CW, AW and trend from y_{p}.

5.2 Conclusion

In order to analyze polar motion observations in the time period spanning from 1960 to 2009 both in x direction and y direction, SSA and MSSA in this thesis is applied to extract CW, AW, trend from polar motion time series.

For new method CSSA, algorithms are straightforward extensions of SSA algorithms to the complex-valued case. With respect to SSA, CSSA can apply on bivariate time series analysis.

New time series $x_{\mathrm{p}} + iy_{\mathrm{p}}$ or $y_{\mathrm{p}} + ix_{\mathrm{p}}$ are combination of polar motion time series in x and y direction. It shows advantage in separating polar motion time series into a slowly varying trend, Chandler wobble, annual wobble and a structureless residual.

Generation of new time series is as $x_{\mathrm{p}} + iy_{\mathrm{p}}$ or $y_{\mathrm{p}} + ix_{\mathrm{p}}$. It doesn't matter whether x_{p} in real part or in imaginary part for x_{p} decomposition. The same as y_{p}.

With respect to SSA and MSSA, the grouping modes are consistent and unique for components reconstruction.

5.3 Outlook

Lag window length is the single parameter of embedding to build trajectory matrix. So it is important to select an optimal window length for SSA, MSSA and CSSA. In the future, window length selection for CSSA is worth study.

A joint analysis CSSA is carried out between x and y direction. CSSA perform well in decomposition polar motion time series into CW, AW and trend. But as it is bi-variate time series in x and y direction, the next step of research is to find out the usefulness in multi-variate time series analysis.

Areas where SSA and MSSA can be applied are very broad: climatology, marine science, geophysics, engineering, image processing, medicine, econometrics (Golyandina et al.,

2001). In the future, CSSA can be used in practical applications such as trend extraction, periodicity detection, seasonal adjustment, smoothing and noise reduction.

Bibliography

Cadzow J. A. (1988). Signal enhancement-a composite property mapping algorithm. IEEE Transactions on Acoustics, Speech, and Signal Processing, 36 (1): 49–62. DOI: 10.1109/29.1488.

Chen Q., van Dam T., Sneeuw N., Collilieux X., Weigelt M., and Rebischung P. (2013). Singular spectrum analysis for modeling seasonal signals from GPS time series. Journal of Geodynamics, 72: 25–35. DOI: 10.1016/j.jog.2013.05.005.

Cui b. (2015). *Application of singular spectrum analysis to EOP time series*.

Dong D, Fang P, Bock Y, Webb F, Prawirodirdjo L, Kedar S, and Jamason P (2006). Spatiotemporal filtering using principal component analysis and Karhunen-Loeve expansion approaches for regional GPS network analysis. Journal of Geophysical Research: Solid Earth, 111 (B3). DOI: 10.1029/2005JB003806.

Forootan E. and Kusche J (2012). Separation of global time-variable gravity signals into maximally independent components. Journal of Geodesy, 86 (7): 477–497. DOI: 10.1007/s00190-011-0532-5.

Ghil M., Allen M., Dettinger M., Ide K, Kondrashov D, Mann M., Robertson A. W., Saunders A, Tian Y, Varadi F, et al. (2002). Advanced spectral methods for climatic time series. Reviews of geophysics, 40 (1). DOI: 10.1029/2000RG000092.

Golyandina N and Stepanov D (2005). SSA-based approaches to analysis and forecast of multidimensional time series. 293: 298.

Golyandina N., Nekrutkin V., and Zhigljavsky A. A. (2001). Analysis of time series structure: SSA and related techniques.

Groth A. and Ghil M. (2011). Multivariate singular spectrum analysis and the road to phase synchronization. Physical Review E, 84 (3): 036206. DOI: 10.1103/PhysRevE.84.036206.

Hassani H. (2007). Singular spectrum analysis: methodology and comparison.

Hassani H., Mahmoudvand R., Zokaei M., and Ghodsi M. (2012). On the separability between signal and noise in singular spectrum analysis. Fluctuation and Noise Letters, 11 (02): 1250014. DOI: 10.1142/S0219477512500149.

Höpfner J. (2003). Chandler and annual wobbles based on space-geodetic measurements. Journal of Geodynamics, 36 (3): 369–381. DOI: 10.1016/S0264-3707(03)00056-5.

Malkin Z. and Miller N. (2010). Chandler wobble: two more large phase jumps revealed. Earth, planets and space, 62 (12): 943–947. DOI: 10.5047/eps.2010.11.002.

Miller N and Malkin Z (2013). Analysis of Polar Motion Variations from 170-year Observation Series. arXiv preprint arXiv:1304.3985.

Mo K. C. (2001). Adaptive Filtering and Prediction of Intraseasonal Oscillations. Monthly Weather Review, 129 (4): 802–817. DOI: 10.1175/1520-0493(2001)129<0802:AFAPOI>2.0.CO;2.

Nekrutkin V. (1996). "Theoretical properties of the" Caterpillar" method of time series analysis". In: *Statistical Signal and Array Processing, 1996. Proceedings., 8th IEEE Signal Processing Workshop on (Cat. No. 96TB10004*. IEEE, pp. 395–397. DOI: 10.1109/SSAP.1996.534899.

Oropeza V. and Sacchi M. (2011a). Simultaneous seismic data denoising and reconstruction via multichannel singular spectrum analysis. Geophysics, 76 (3): V25–V32. DOI: 10.1190/1.3552706.

Oropeza V. and Sacchi M. (2011b). Simultaneous seismic data denoising and reconstruction via multichannel singular spectrum analysis. Geophysics, 76 (3): V25–V32. DOI: 10.1190/1.3552706.

Rangelova E, Van der Wal W, Braun A, Sideris M., and Wu P (2007). Analysis of Gravity Recovery and Climate Experiment time-variable mass redistribution signals over North America by means of principal component analysis. Journal of Geophysical Research: Earth Surface, 112 (F3). DOI: 10.1029/2006JF000615.

Read P. (1993). Phase portrait reconstruction using multivariate singular systems analysis. Physica D: Nonlinear Phenomena, 69 (3): 353 –365. DOI: 10.1016/0167-2789(93)90099-M.

Smylie D., Henderson G. A., and Zuberi M. (2015). Modern observations of the effect of earthquakes on the Chandler wobble. Journal of Geodynamics, 83: 85–91. DOI: 10.1016/j.jog.2014.09.012.

Torge W. and Müller J. (2012). Geodesy. Walter de Gruyter.

Trickett S. et al. (2008). "F-xy Cadzow noise suppression". In: *2008 SEG Annual Meeting*. Society of Exploration Geophysicists.

Vautard R. and Ghil M. (1989). Singular spectrum analysis in nonlinear dynamics, with applications to paleoclimatic time series. Physica D: Nonlinear Phenomena, 35 (3): 395–424. DOI: 10.1016/0167-2789(89)90077-8.

Von Storch H. and Zwiers F. W. (2002). *Statistical analysis in climate research*.

Vondrák J. and Richter B. (2004). International Earth Rotation and Reference Systems Service (IERS) web: www. iers. org. Journal of Geodesy, 77 (10-11): 585–678.

Wang G., Liu L., Su X., Liang X., Yan H., Tu Y., Li Z., and Li W. (2016). Variable Chandler and Annual Wobbles in Earth's Polar Motion During 1900–2015. Surveys in Geophysics, 37 (6): 1075–1093.

Zhigljavskya A., Hassania H., and Heravib S. (2008). Forecasting European Industrial Production with Multivariate Singular Spectrum Analysis.

Zotov L. and Shum C. (2010). "Multichannel singular spectrum analysis of the gravity field data from GRACE satellites". In: *AIP Conference Proceedings*. Vol. 1206. 1. AIP, pp. 473–479. DOI: 10.1063/1.3292557.

List of Figures

List of Tables